

A new bipolar ice core record of volcanism from WAIS Divide and NEEM and implications for climate forcing of the last 2000 years

Michael Sigl,¹ Joseph R. McConnell,¹ Lawrence Layman,¹ Olivia Maselli,¹
 Ken McGwire,¹ Daniel Pasteris,¹ Dorthe Dahl-Jensen,² Jørgen Peder Steffensen,²
 Bo Vinther,² Ross Edwards,³ Robert Mulvaney,⁴ and Sepp Kipfstuhl⁵

Received 31 July 2012; revised 29 October 2012; accepted 25 November 2012; published 7 February 2013.

[1] Volcanism is a natural climate forcing causing short-term variations in temperatures. Histories of volcanic eruptions are needed to quantify their role in climate variability and assess human impacts. We present two new seasonally resolved, annually dated non-sea-salt sulfur records from polar ice cores—WAIS Divide (WDC06A) from West Antarctica spanning 408 B.C.E. to 2003 C.E. and NEEM (NEEM-2011-S1) from Greenland spanning 78 to 1997 C.E.—both analyzed using high-resolution continuous flow analysis coupled to two mass spectrometers. The high dating accuracy allowed placing the large bi-hemispheric deposition event ascribed to the eruption of Kuwae in Vanuatu (previously thought to be 1452/1453 C.E. and used as a tie-point in ice core dating) into the year 1458/1459 C.E. This new age is consistent with an independent ice core timescale from Law Dome and explains an apparent delayed response in tree rings to this volcanic event. A second volcanic event is detected in 1453 C.E. in both ice cores. We show for the first time ice core signals in Greenland and Antarctica from the strong eruption of Taupo in New Zealand in 232 C.E. In total, 133 volcanic events were extracted from WDC06A and 138 from NEEM-2011-S1, with 50 ice core signals—predominantly from tropical source volcanoes—identified simultaneously in both records. We assess the effect of large bipolar events on temperature-sensitive tree ring proxies. These two new volcanic records, synchronized with available ice core records to account for spatial variability in sulfate deposition, provide a basis for improving existing time series of volcanic forcing.

Citation: Sigl, M., et al. (2013), A new bipolar ice core record of volcanism from WAIS Divide and NEEM and implications for climate forcing of the last 2000 years, *J. Geophys. Res. Atmos.*, 118, 1151–1169, doi:10.1029/2012JD018603.

1. Introduction

1.1. Volcanoes and Climate Forcing

[2] Volcanic eruptions are an important natural cause of climate change. Large volcanic eruptions inject sulfur gases into the stratosphere, which convert to sulfate aerosols. The radiative and chemical effects of this aerosol cloud results in cooling of the surface and lower troposphere by scattering solar radiation [Cole-Dai, 2010; Robock, 2000]. This parasol

effect on climate was held responsible for numerous cold spells in Earth and human history: Volcanic winters following super eruptions were thought to reduce human population, affect vegetation cover, and alter development of human cultures [Ambrose, 1998; Riede, 2008; Williams et al., 2009] in prehistoric times. The climate effects of eruptions in historic times are recorded in proxy archives such as tree ring records [Jones, Briffa, and Schweingruber, 1995; Salzer and Hughes, 2007] and ice core records [Cole-Dai et al., 2009; Larsen et al., 2008; Zielinski et al., 1994]. These effects also are described in written records [Oppenheimer, 2003a; Thordarson and Self, 2003].

[3] Uncertainty in the magnitude of past volcanic activity strongly limits estimates of climate sensitivity, defined as the equilibrium mean temperature changes following a doubling of atmospheric carbon dioxide concentrations [Hegerl, Crowley, Hyde, and Frame, 2006], which in turn is a key number in the discussion in mitigating climate change through policy decisions.

[4] Only for the last 150 years are reliable estimates of stratospheric aerosol optical depth available [Sato, Hansen, McCormick, and Pollack, 1993]. Before 1850, volcanic forcing indices rely on ice core based reconstructions using sulfate and acidity deposition series extracted from predominantly

¹Division of Hydrologic Sciences, Desert Research Institute, Reno, Nevada, USA.

²Center for Ice and Climate, Niels Bohr Institute, University of Copenhagen, Copenhagen, Denmark.

³Department of Physics, Curtin University, Perth, Australia.

⁴British Antarctic Survey, Madingley Road, High Cross, Cambridge, Cambridgeshire, United Kingdom.

⁵Alfred-Wegener-Institut für Polar- und Meeresforschung, Bremerhaven, Germany.

Corresponding author: M. Sigl, Desert Research Institute, 89512 Raggio Parkway, Reno, NV 89512, USA. (msigl@dri.edu)

©2012. American Geophysical Union. All Rights Reserved.
 2169-897X/13/2012JD018603

polar ice cores [Gao, Oman, Robock, and Stenchikov, 2007; Zielinski, 1995]. The most comprehensive index of volcanic forcing to date is that of Gao, Robock, and Ammann (2008) covering the last 1500 years. They used 54 ice core records from Antarctica and Greenland showing volcanic eruptions, thereby providing more spatial coverage than any previous estimates for volcanic forcing. Not all of these records are based on sulfate (the preferred parameter due to the direct link to aerosol optical depth), however, and only a few records cover more than the last 500 years. For many Antarctic ice core records, dating accuracy also is limited by relatively low annual accumulation rates. This hampers assignment of large-scale stratospheric tropical eruptions that are known to have a larger global-scale radiative effect than volcanic eruptions closer to the poles where deposition is restricted to one hemisphere [Robock, 2000].

[5] Here we present two new ice core records, one from Greenland and one from Antarctica, that cover most of the last 2000 years, based on high-resolution non-sea-salt sulfur (nssS) measurements. The dating precision of these seasonally resolved and annually dated records is unique for a noncoastal ice core site in Antarctica. Similar dating precision only could be achieved for coastal sites such as Law Dome but which are characterized by a high background flux in marine biogenic sulfate that is unfavorable to detection of volcanic fallout in ice cores. The Western Antarctic Ice Sheet Divide (WAIS Divide) is ideally suited to obtain a well dated volcanic record as the relatively high accumulation rates. Combined with high-resolution continuous flow analysis (CFA) used here, this allows for determination of an accurate timescale. At the same time due to the large distance to the ocean, WAIS Divide background levels in nonvolcanic sulfate are low, allowing detection of more volcanic events than in previous Antarctic ice core records. Together with a new high-resolution volcanic record from Greenland, a more complete precisely dated inventory of eruptions and their potential source areas during the last 2000 years can be established, providing a basis for refining existing volcanic forcing indices.

1.2. Volcanoes as Time Markers in Ice Core Dating

[6] In addition to being a proxy of past climate forcing, the record of volcanism in ice cores provides age information to establish timescales for ice core based records. Strong explosive eruptions usually inject high amounts of sulfur into the stratosphere. Depending on the source of the eruption, these aerosols are deposited regionally, hemispherically, or globally. Because of the widespread distribution and deposition of sulfate aerosols from explosive volcanism, sulfate layers detected in ice cores can serve as time markers. These time markers have an absolute age, if the calendar age of the eruption is known. For example, the eruptions of Agung (Indonesia, 1963 C.E.), Krakatoa (Indonesia, 1883 C.E.), Tambora (Indonesia, 1815 C.E.), and Huaynaputina (Peru, 1600 C.E.) all localized in the tropics, are widely used as time markers for ice core chronologies [Gao et al., 2008]. For Greenland, additional time markers are available from various eruptions that took place in Iceland (e.g., Katla, Hekla), or in Alaska and Kamtschatka [Oladottir, Larsen, and Sigmarsson, 2011; Thordarson and Larsen, 2007; Zielinski et al., 1994]. The sulfate layer of the Laki eruption (Iceland, 1783 C.E.)

is a prominent time marker in ice core records detected in Greenland, Svalbard, and the Alps [Jenk et al., 2009; Kekonen, Moore, Peramaki, and Martma, 2005; Thordarson and Self, 2003]. Another signal detected in Greenland ice cores is from the eruption of Vesuvius (Italy, 79 C.E.) reported by Roman historians. After confirmation of the source volcano by tephra analysis, use of this volcano time marker significantly reduced age uncertainty for the underlying ice core chronology Greenland Ice Core Chronology “GICC05” [Rasmussen et al., 2006; Vinther et al., 2006].

[7] While many of the Icelandic eruptions back into the middle ages are associated with reliable eruption dates reported by historic witnesses, this is not true for the majority of eruptions that took place in remote areas of the tropics and the Southern Hemisphere [Simkin and Siebert, 1994]. Nevertheless, two additional time markers from large stratospheric eruptions in the tropics are used as tie-points for development of ice core chronologies: an unknown eruption in 1258 [Oppenheimer, 2003a], the largest volcanic event of the last millennium, and the signal in 1452/1453 associated with the eruption of Kuwae in Vanuatu [Gao et al., 2006], the largest volcanic event of the last millennium for most of the Antarctic ice core records. Various volcanic timescales in Antarctica were tied to this 15th century time marker [Delmas, Kirchner, Palais, and Petit, 1992; Ferris, Cole-Dai, Reyes, and Budner, 2011; Jiang et al., 2012; Sommer, Wagenbach, Mulvaney, and Fischer, 2000; Stenni et al., 2002]. Here we provide additional evidence from independent, well dated ice core records from both hemispheres showing that this major stratospheric eruption actually occurred 6 years later than the accepted age of 1452/1453 C.E. We analyze consequences in climate response for the corrected underlying timescale using temperature sensitive tree ring series.

2. Methods

2.1. WDC06A and NEEM-2011-S1 Core Recovery

[8] As part of the WAIS project, a deep ice core was drilled at 79.47°S/112.09°W (1759 m a.s.l.). The drilling was finished in 2011 to a depth of 3405 m. Here we discuss results of the upper 579 m of the main ice core (“WDC06A”). A well-defined ice flow regime [Morse, Blankenship, Waddington, and Neumann, 2002] and modern accumulation rates of $200 \pm 34 \text{ kg m}^{-2} \text{ a}^{-1}$ [Banta, McConnell, Frey, Bales, and Taylor, 2008] make this site a unique archive for high-resolution chemical analysis. A shallow ice core “WDC05Q” drilled at WAIS Divide in 2005 was used to validate results during the overlap period of 1521 and 2005 C.E.

[9] Within the NEEM drilling project, a 411 m deep ice core (“NEEM-2011-S1” in the following “NEEM S1”) was drilled in 2011 at 77.45°N 51.06°W in northwest Greenland. The drill site was close to the main borehole where recovery of a 3538 m long ice core reaching back into the previous interglacial was finished in the same year. Annual precipitation of $210 \text{ kg m}^{-2} \text{ a}^{-1}$ is comparable to that of the WAIS Divide ice core, allowing for accurate annual-layer interpretation. We use continuously measured nssS in the nearby Humboldt ice core at 78.53°N/56.83°W (1985 m a.s.l.) to validate ice core signals detected in the NEEM S1 record between 1154 and 1995 C.E.

2.2. Laboratory Analysis

[10] The WAIS Divide ice core samples were initially processed at the National Ice Core Laboratory (NICL, Colorado). Chemical and elemental measurements were performed using 1 m long ice sticks (30x30 mm) at the Ultra Trace Chemistry Laboratory at the Desert Research Institute (DRI). Core quality was excellent throughout most of the 579 m. By using a CFA system coupled to two inductively coupled plasma mass spectrometers (ICPMS) and a single particle soot photometer (SP2) for black carbon (BC) determination, a wide variety of 25 elements (e.g., Na, S, Br, Ca, Fe) and various chemical species (e.g., NO_3^- , NH_4^+ , H^+) can be quantified simultaneously with low detection limits and an effective sampling resolution of ~1 cm. Details of the analytical setup are given elsewhere [Bisiaux *et al.*, 2012; McConnell, Lamorey, Lambert, and Taylor, 2002; McConnell *et al.*, 2007; Pasteris, McConnell, and Edwards, 2012].

[11] The dual ICPMS system allowed for duplicate measurements on certain parameters (e.g., Na, Ce, Sr, Al, Pb) for quality control and simultaneous determination of a broad spectrum of elements. As CFA is a destructive method, a dual system provides redundancy in case of instrument failure. To further assess reproducibility, 10% of all ice core samples were reanalyzed using parallel replicate melter sticks. Overall quantification uncertainties for the elements discussed in detail in this paper are less than $\pm 5\%$. More details on recovery, accuracy, and reproducibility of the analytical setup are given by McConnell *et al.*, 2007, 2002.

[12] The ice core samples from NEEM S1 were processed at the Desert Research Institute in the same way. The quality of the ice cores was excellent except for a section between 323 and 332 m where the cores were broken during transport. Those data gaps in the NEEM S1 sulfur record were filled using sulfate concentrations determined by fast ion chromatography [Littot *et al.*, 2002] in the main NEEM ice core. Sulfate concentration and sulfur concentration are in close agreement as determined for time periods of overlapping data with background sulfate concentrations being 3 ng/g lower than total sulfur concentrations. Annual average concentrations agree with $r=0.84$ ($N=230$, $p<0.001$). Deposition fluxes determined for common volcanic events in both data sets agree with $r=0.80$ ($N=34$, $p<0.001$). In total 3.3% of the NEEM volcano record is based on sulfate concentration from the parallel main core. As with the WAIS Divide samples, replicate cores have been analyzed for 10% of the NEEM S1 core over the entire 411 m length.

2.3. Ice Core Dating

[13] Various parameters measured in ice cores exhibit seasonal cycles that can be used to interpret annual layers and determine an absolute age for the corresponding ice depth [Rasmussen *et al.*, 2006]. In Greenland as in Antarctica, individual parameters peak in different seasons. While sea salt tracers usually have their annual maxima in winter months, dust transport is generally highest in spring and organic tracers such as NH_4^+ reach highest concentrations during summer months [Kuramoto *et al.*, 2011; Rasmussen *et al.*, 2006]. High-accumulation ice core sites in Antarctica, such as Law Dome, could therefore be successfully dated by annual layer counting [Palmer *et al.*, 2001].

[14] CFA systems also have been proven to allow annual layer counting for low accumulation ice core sites in Antarctica such as Dronning Maud Land [Traufetter, Oerter, Fischer, Weller, and Miller, 2004] and the South Pole [Ferris *et al.*, 2011]. Compared to these sites, the accumulation rate at WAIS Divide is higher by a factor of three and comparable to major deep ice core sites in Greenland (e.g., NorthGRIP, NEEM). Therefore, high accuracy annual dating at WAIS Divide is feasible, as has been demonstrated for the last 500 years using a comparable analytical setup to analyze two shorter ice cores (“WDC05A,” “WDC05Q”) drilled at WAIS Divide in 2005 [Cole-Dai *et al.*, 2009].

[15] A multiparameter dating approach based on manual interpretation of various parameters showing strong annual cycles is used in this work. Biogenic emissions and sea spray from the ocean, continental dust, and emissions from biomass burning all exhibit a strong seasonality in source strength and transport [Kuramoto *et al.*, 2011; Weller *et al.*, 2008]. Their specific fluxes to the ice core sites can be deduced from concentration records of sulfur (marine biogenic emissions), sodium and chlorine (sea spray), aluminum, iron, calcium (continental dust), and black carbon or ammonium (biomass burning). The independence of these various coregistered parameters is important since individual parameters might be masked (e.g., natural annual cycles in S or H^+ from marine biogenic emissions can be masked by large volcanic acid deposition).

[16] We primarily based interpretation of annual signals for the WDC06A and NEEM S1 ice cores on concentration records of sodium (Na), nssS, BC, non-sea-salt calcium (nssCa), and the ratio of nssS/Na. Additionally, time series of ammonium, bromine, lead, acidity, and conductivity were included, if the interpretation of the above parameters were not clear. For the few sections of problematic core quality that could not be measured at DRI (bad core breaks, broken cores), the annual interpretation relied on electrical conductivity measurements (ECM) and dielectric profiling (DEP) performed before shipment to DRI [Moore, 1993; Taylor *et al.*, 2004; Taylor, Alley, Lamorey, and Mayewski, 1997]. The quality of those measurements is good, and the poor quality of most sections was only a result of the shipment process. All reported ages in this work are C.E. (A.D.) unless stated otherwise.

[17] The timescales of the WDC06A and NEEM S1 cores have been fixed to volcanic time markers. In addition to the volcanic event of 1259 ± 1 —an outstanding and unique signal in ice cores from both hemispheres with a well-constrained age estimate from Greenland [Oppenheimer, 2003b]—only volcanic signals from historically documented eruptions have been used to tie the absolute ages. For the WAIS Divide core, these include tropical eruptions of Krakatoa (1883), Tambora (1815), and Huayinaputina (1600). A detailed study of the volcanic imprint from the Tambora eruption in WAIS Divide is reported by Cole-Dai *et al.* (2009). For NEEM S1, additional eruptions with sources in the Northern Hemisphere were used to constrain the annual layer interpretation: Katmai (1912), Laki/Grimsvotn (1783), Bárðarbunga (1477), Hekla (1104), Eldgjá (934 ± 2) [Thordarson and Larsen, 2007], and Vesuvius (79) [Vinther *et al.*, 2006].

[18] Uncertainty in an annually dated ice core timescale can be due to imperfect core stratigraphy; core or data loss during drilling, handling, sampling and measurements;

insufficient measuring resolution; and misinterpretation of the annual layer record [Rasmussen *et al.*, 2006]. For the upper part of NEEM S1 and WDC06A data presented here, layer thinning was negligible, thus giving the records sufficient measuring resolution. Uncertainty due to disturbed stratigraphy (e.g., through melting or erosive loss of snow accumulation) was minimized by choice of the drill sites and their relatively high annual snow accumulation. Therefore, the major source of uncertainty for these sections of the ice cores lies in the possibility of an erroneous interpretation of the annual layer record. While the vast majority of the annually interpreted layers are expressed clearly by each of the individual parameters, there were occasionally cases that allowed for alternative dating interpretations. To quantify this uncertainty, we followed two independent approaches.

[19] 1. We compared the annual layer record with a reinterpretation that is using an automated peak identification algorithm developed and applied for annual layer counting of Antarctic ice core profiles [McGwire, Taylor, Banta, and McConnell, 2011]. We performed the analysis independently from volcanic tie points and separately for the parameters Na, nssS/Na, and BC.

[20] 2. We contrast the obtained ages of major volcanic signals with independent annual layer counted ice core records from Law Dome, Dronning Maud Land, South Pole, and NorthGRIP [Traufetter *et al.*, 2004; Ferris *et al.*, 2011; Plummer *et al.*, 2012].

2.4. Volcanic Sulfate Flux Calculation

[21] We corrected total S concentrations for the sea salt sulfur contribution using Na concentrations as a sea salt tracer and assuming a sulfur to sodium ratio in bulk sea water of 0.084 [Bowen, 1979]. Annual average concentrations of non-sea-salt sulfur (nssS) were calculated between the maxima of nssS/Na for WDC06A and between the minima of nssS/Na for NEEM S1, representing approximately January of each calendar year. To display the highly resolved data in the time domain, we display the sulfur record also as “monthly averages” without claiming monthly precision in the dating. For this we assume uniform snow deposition throughout the year which is corroborated by field measurements from Greenland and Antarctica, at least for the most recent time periods [Kuramoto *et al.*, 2011; Steig *et al.*, 2005].

[22] The nssS ice core record is due to atmospheric deposition from primarily two different sources: a flux from marine biogenic sulfur deposition (representing natural background, or noise) is superimposed by sporadic deposition of volcanic, excess sulfur (the signal to be extracted). The strength and variability of the natural background deposition therefore determines the signal-to-noise ratio, thus favoring continental ice core sites for volcanic reconstructions over coastal ice core sites. A majority of ice core based volcanic records is derived from inland sites of the Antarctic and Greenland ice sheets [Basile, Petit, Tournon, Grousset, and Barkov, 2001; Castellano *et al.*, 2005; Ferris *et al.*, 2011; Jiang *et al.*, 2012; Zielinski *et al.*, 1994]. Ice cores from coastal sites have proved to be valuable archives of past volcanism, if a second independent parameter unique for biogenic sulfur emissions (such as MSA) is used in the detection process [Traufetter *et al.*, 2004]. For detection of volcanic signals

in sulfur or sulfate ice core records with an approximately constant natural background, a variety of statistical methods have been applied in the past [Castellano *et al.*, 2005; Gao *et al.*, 2007; Kurbatov *et al.*, 2006; Traufetter *et al.*, 2004]. Detailed sensitivity studies of how the choice of the volcano detection procedure influences detection and quantification of volcanic deposition has been performed for various ice core records [Ferris *et al.*, 2011; Gao *et al.*, 2008]. These studies demonstrated that the results were robust for the different methods in detecting and quantifying at least medium to large-scale volcanic events, which are most important in terms of their climate impact.

[23] To extract the volcanic signals from the nssS ice core records of NEEM S1 and WDC06A, we used a methodology adapted from Traufetter *et al.* (2004) as follows.

[24] 1. As a measure of the natural background, we applied a 31 year running median (RM) filter on the annually averaged nssS time series.

[25] 2. The median of absolute deviation (MAD) provided a robust measure of variability in the data in the presence of volcanic peaks and long-term variations in atmospheric background. An annual nssS value was assumed to be volcanic if it exceeded $3 \times \text{MAD}$ above the RM.

[26] 3. The filter length of RM to approximate background variations and the detection threshold value of $3 \times \text{MAD}$ were chosen empirically and validated using volcanic signals of well-known historic eruptions. Similar thresholds and filter length are used by Ferris *et al.* (2011) and Gao *et al.* (2006).

[27] 4. Finally, we calculated total volcanic sulfate deposition related to each detected volcanic eruption by integration of the part of the volcanic nssS peak above the reduced 31 year running median (RRM), calculated after excluding all detected volcanic peaks from the data set. Thereby, we assumed that total sulfur during deposition consisted of sulfate aerosols, the final product during atmospheric oxidation processes.

[28] 5. As the uncertainty of the volcanic deposition flux is strongly determined by variations in the natural background, we estimated its uncertainty by calculating a 31 year running standard deviation of the RRM describing the nonvolcanic background.

[29] We present two independent records of volcanic deposition and, given the high dating accuracy obtained for the Antarctic WDC06A core, we were able to identify global eruptions responsible for global-scale climate effects during the last 2000 years. We further investigated the temperature response of these new volcanic aerosol records by comparing to selected temperature sensitive climate proxies.

3. Results

3.1. WDC06A Timescale and Uncertainty

[30] Various parameters showed pronounced annual variability providing the basis for annually dating the ice core record. The most pronounced annual variations are in records of Na (a sea salt tracer, peaking in austral winter months), BC (a biomass burning tracer peaking in early summer), and nssS (a tracer for marine biogenic emissions peaking in austral summer). A 10 m long section covering

the time period 1539–1586 illustrates the strength and consistency of the annual signals we used for dating (Figure 1). Using various concentration records that derive from different sources and peak in different seasons helps in interpretation of ambiguous annual signals. For example, if a multiyear volcanic sulfur event is superimposed upon the annual cycle in marine biogenic sulfur, annual dating can be performed on the basis of BC cycles. The BC record is derived from particle measurements and is thus conservative against potential effects that large acid events from volcanoes might have on the chemistry signals of an ice core.

[31] Using the four well dated volcanic markers (1963, 1883, 1815, 1600) and the 1259 event to constrain the annual layer interpretation, we established a 2415 year long record. The thinning corrected average annual layer thickness was $0.23 (\pm 0.04)$ m water equivalent.

[32] For most of the ice core, the number of manually picked years using the multiparameter approach agreed well with the number of years estimated from the automated picking approach using BC as the dating parameter. The automated approach estimated 10 additional years (+0.4%) in total. The difference between the two dating techniques was only 3 years (0.2%) between 674 and 2006 and 7 years (0.6%) between 426 BCE and 674. The higher uncertainty in the lower part of the record is due to some sections of poor sample quality leading to small data gaps and reduced quality in the chemistry measurements. As a conservative estimate of age uncertainty between volcanic time markers, we therefore assume a relative counting error of 0.5% for the last 1000 years and up to 1% before that (Figure 3).

[33] A recent record from Law Dome (Dome Summit South, DSS) is the ice core record with the highest dating accuracy covering the last 2000 years in Antarctica [Plummer *et al.*, 2012]. The largest volcanic events are recorded in this high accumulation coastal ice core record from East Antarctica, allowing comparison to the timescale of WDC06A. During all common volcanic events between

1000 and 2006, both timescales agree within ± 1 year. The maximum age difference for the entire 2000 years is 3 years at around 425. Within the individual counting errors, both independent ice core timescales are therefore identical and in their accuracy comparable to Greenland ice core timescales (Figure 2).

[34] The two annual-layer-counted timescales for the low accumulation sites of Dronning Maud Land, DML B32 [Traufetter *et al.*, 2004] and South Pole, SP04 [Ferris *et al.*,

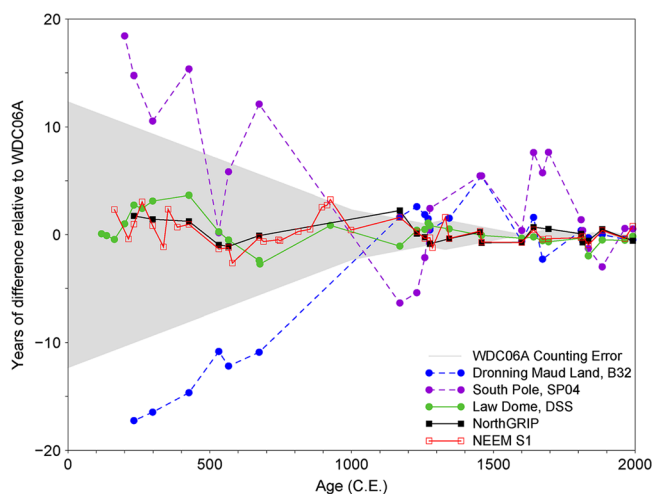


Figure 2. Relative age difference between the new independent timescale of WAIS Divide, WDC06A to annually dated ice cores of the South Pole, SP04 [Ferris *et al.*, 2011], Dronning Maud Land, B32 [Traufetter *et al.*, 2004], Law Dome, DSS [Plummer *et al.*, 2012], NEEM S1 (this study), and NorthGRIP [Plummer *et al.*, 2012] using individual ice core ages of common large volcanic events. Grey shading indicates the cumulative “counting” uncertainty in interpretation of annual signals in WDC06A.

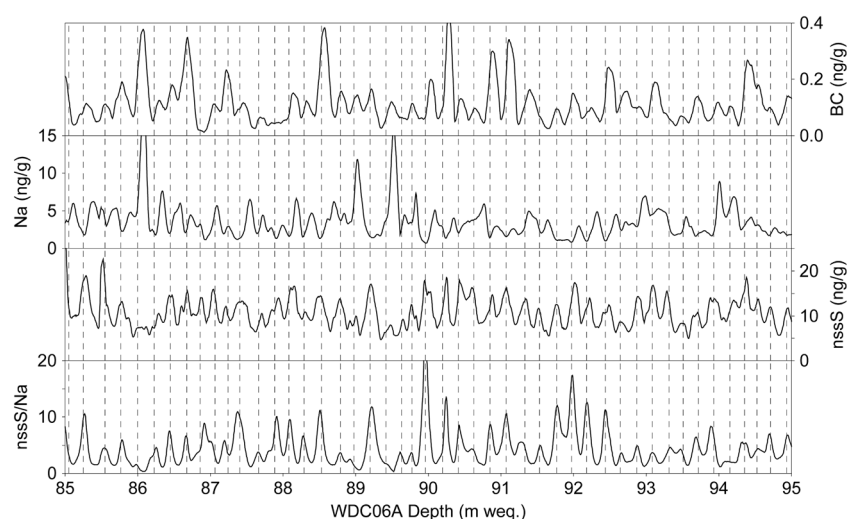


Figure 1. High-resolution annual layer dating of a 10 m water-equivalent (m weq.) long section of WDC06A, representing 1538–1584 C.E., using a multiparameter approach. Concentration records of Na, nssS, BC, and nssS/Na are displayed, with black dashed lines indicating the assigned years. Additional parameters used for interpretation of seasonal signals that are not shown include Ca, NH_4^+ , Br, Pb(208), acidity, and conductivity.

2011] agree within ± 20 years during the last 2000 years to the WDC06A timescale.

3.2. NEEM-2011-S1 Timescale and Uncertainty

[35] Similar to the dating of WDC06A, annual layers were identified for seasonal signals of nssS, nssS/Na, Na, nssCa, and BC for NEEM S1 (Figure 3). Since the annual cycles in nssS and BC were superimposed by anthropogenic pollution for the last 100 years [McConnell *et al.*, 2007], sea salt and dust tracers were the primary dating parameters for this time period.

[36] The thinning corrected average annual layer thickness was $0.21 (\pm 0.04)$ m water equivalent comparable to the Antarctic WDC06A record, resulting in identification of 1932 annual layers. In addition to the bi-hemispheric volcanic events used for the WDC06A timescale, the absolute ages were constrained by additional historic volcanic events in 1783, 1477, 1105, 934 ± 2 , and 79. To be consistent with the high precision GICC05 Greenland ice core timescale, we used additional volcanic events from NorthGRIP [Plummer *et al.*, 2012] to guide the annual layer identification process for ambiguous layers. Thus, NEEM S1 is closely linked to NorthGRIP and thereby to the GICC05 timescales within ± 1 year during all major common volcanic events. This is at the cost of independence of the NEEM S1 ice core timescale. The decision for consistency at a cost of independence is justified given the high dating accuracy of the GICC05 timescale, which does not exceed ± 2 years in the last 2000 years [Larsen *et al.*, 2008; Vinther *et al.*, 2006]. By choosing this dating technique, however, the NEEM S1 timescale cannot be used to validate the accuracy of the GICC05 timescale.

3.3. WAIS Divide Volcanic nssS Record (408B.C.E.–2006)

[37] Figure 4a displays the nssS record derived from the WDC06A and WDC05Q ice cores. The median of the annually averaged nssS concentration for WDC06A was 12.1 ng/g with 50% of the data ranging between 10.5 and 14.3 ng/g . The flux of the natural marine biogenic sulfate

deposition and its variability was low ($8 \pm 2 \text{ kg km}^{-2}$). This background was superimposed by numerous volcanic sulfate deposition events. In total, 133 volcanic events were detected depositing 1840 kg km^{-2} sulfate during the last 2400 years (Table 1). 59 volcanic signals with a flux of $>10 \text{ kg km}^{-2}$ and quantification uncertainties $<20\%$ were recorded. All volcanic events in WDC06A were verified by WDC05Q in the period of overlap, with flux estimates being highly reproducible with $r=0.95$ ($N=23$, $p < 0.001$). Deposition estimates for most of the major events agreed closely with independent estimates from other ice core sites and Antarctic composite data (Table 2).

[38] For the time period 180–2000, covered by the annually dated ice cores of the South Pole and Dronning Maud Land, about 50% more events with $>10 \text{ kg km}^{-2}$ sulfate were detected at WAIS Divide compared to other volcanic records. For South Pole (90°S) this probably was due to reduced flux to the high latitudes, while the difference to Law Dome and Dronning Maud Land was due to enhanced marine biogenic sulfate deposition at these coastal sites masking the signal of some volcanic eruptions. The majority of the large volcanic signals were recorded in all of these Antarctic ice cores, however, allowing evaluation of spatial aspects of volcanic sulfate deposition (Table 2) and cross comparisons of individual timescales (Figure 2).

[39] The largest single volcanic event in the WDC06A record was from a mid-15th century eruption previously ascribed to Kuwae, Vanuatu ($104 \text{ kg km}^{-2} \text{ SO}_4^{2-}$). The age, signal, and consequences of this eruption are described in detail later. The unknown event of 1259 ($80 \text{ kg km}^{-2} \text{ SO}_4^{2-}$) and the eruption of Tambora in Indonesia in 1815 ($87 \text{ kg km}^{-2} \text{ SO}_4^{2-}$) rank next. Periods of enhanced volcanism in Antarctica as indicated by the number of events and their aerosol load were in the 19th, 17th, and 13th centuries, while volcanic activity was low during the 18th and 11th centuries.

3.4. NEEM-2011-S1 Volcanic nssS Record (78–1999)

[40] Figure 4b displays the nss sulfur record derived from the NEEM S1 and Humboldt ice cores. The median of the annually averaged nssS concentration for NEEM S1 was

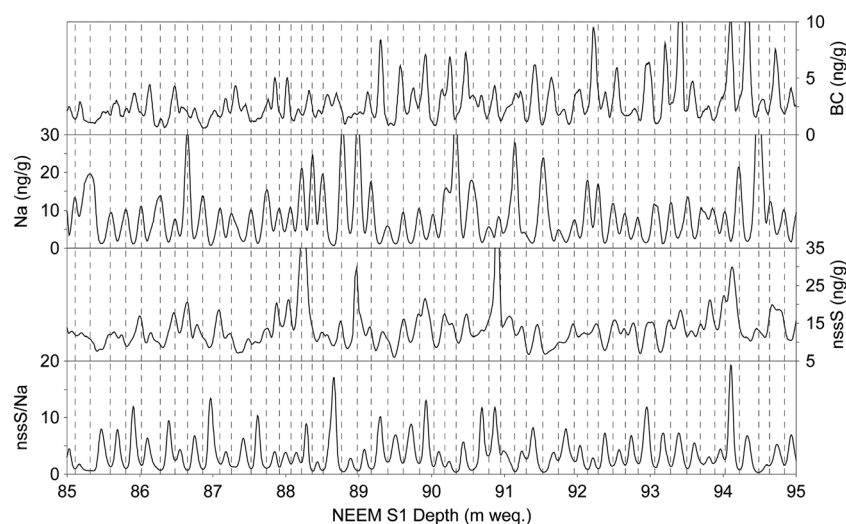


Figure 3. High-resolution annual layer dating of 10 m weq. long section of NEEM S1, representing 1534–1584 C.E., using a multiparameter approach. Concentration records of Na, nssS, BC, and nssS/Na are displayed, with black dashed lines indicating the assigned years. Additional parameters used for interpretation of seasonal signals that are not shown include Ca, NH_4^+ , Br, Pb(208), acidity, and conductivity.

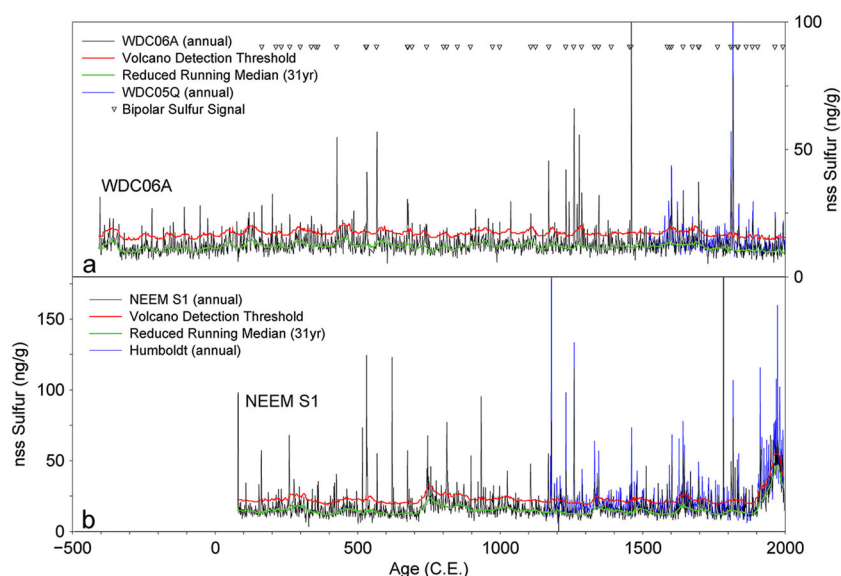


Figure 4. Annually averaged non-sea-salt sulfur (nssS) concentration records from (a) WAIS Divide: WDC06A (black) and WDC05Q (blue) and (b) from Greenland: NEEM S1 (black) and Humboldt (blue). The volcano detection threshold for the selection of volcanic events (red) is based on the background variability of nssS concentration determined by a 31 year running median. The reduced running median (green) displays the nonvolcanic variability of nssS after removal of detected volcanoes in the data set. Triangles indicate bipolar sulfur signals.

15.3 ng/g with 50% of the data ranging between 12.8 and 19.2 ng/g. Marine biogenic sulfate deposition, underlying the volcanic sulfate events, was $9 \pm 2 \text{ kg km}^{-2}$. In total, 138 volcanic events were detected depositing 2970 kg km^{-2} sulfate since 78 C.E. (Table 1). 86 volcanic signals with a flux of $>10 \text{ kg km}^{-2}$ and quantification uncertainties $<20\%$ were recorded. All major volcanic events between 1170 and 1996 in NEEM S1 also were detected in the nearby Humboldt ice core with flux estimates comparable with $r=0.64$ ($N=55$, $p < 0.001$). The differences in sulfate flux between these sites probably reflect spatial variability in deposition. Flux estimates for most of the major events agreed closely with independent estimates from other ice core sites and Greenland composite data (Table 2). The number of volcanoes detected in the NEEM S1 record was in agreement with existing volcanic records from Greenland [Bigler *et al.*, 2002; Gao *et al.*, 2008; Zielinski *et al.*, 1994] during the last 1000 years while during the first millennium more volcanic events were recorded in NEEM S1 (e.g., in 793, 811, 816, 971, and 976) than in other ice core records.

[41] The largest single volcanic events in the NEEM S1 record were from the eruptions of Laki (1783) and Eldgjá (934 ± 2) in Iceland, followed by an event in 619, the historical eruption of Vesuvius (79), and the signal of 1259. Periods of high volcanic sulfate aerosol deposition in Greenland were in the 19th, 13th, and 9th centuries, while volcanic activity was reduced in the 16th, 11th, and 4th centuries.

3.5. Bipolar Signals

[42] Bipolar signals were predominantly from strong volcanic eruptions near the tropics injecting large amounts of SO_2 into the stratosphere leading to subsequent global fallout of sulfate aerosols [Robock, 2000]. A stratospheric pathway of sulfate aerosols can be deduced from sulfur

isotopes [Savarino, Romero, Cole-Dai, Bekki, and Thiemens, 2003], while here we deduced a stratospheric pathway and a tropical eruption source from the high dating precision of the underlying Greenland and Antarctic ice core timescales.

[43] From 1000 to 2000, a total number of 25 signals were detected at the same time in NEEM S1 and WDC06A. These were attributed to known or unknown tropical source volcanoes (Table 1). A bipolar volcanic record from NorthGRIP and Law Dome displays only 16 bi-hemispheric events, while the volcanic forcing index by Gao *et al.* (2008) shows 23 bi-hemispheric eruptions. From 500 to 1000, there were 16 signals assumed to derive from large tropical eruptions in the NEEM S1 and WDC06A records while there were only three events detected in the combined NorthGRIP and Law Dome records [Plummer *et al.*, 2012] and eight in the volcanic forcing index by Gao *et al.* (2008). Before 500, nine isochronic signals were found in the NEEM S1 and WDC06A volcano chronology, among them the signal believed to match the strong eruption of Taupo, New Zealand (see section 4.2), with four of them confirmed by the NorthGRIP and Law Dome records.

[44] In total, 50 bi-hemispheric events from predominantly strong tropical volcanic eruptions were recorded in the new combined record which compares to 31 [Gao *et al.*, 2008] and 23 bi-hemispheric events [Plummer *et al.*, 2012] from existing volcano records (Figure 5). This difference is explained by a combination of high dating accuracy and the signal-to-noise ratio of the underlying sulfur records.

[45] Synchronicity of deposition in both hemispheres is an indication of a stratospheric event and a tropical volcano source only, but not explicit proof of such. Coincidence of two independent events in both hemispheres seems a possible explanation for a bi-hemispheric signal, although this case might be rare. However, some of the events only detected in

Table 1. Volcanic Sulfate Deposition for WDC06A and NEEM S1 Ice Core Records^a

Volcano, Region	WDC06A			NEEM S1		
	Start Date ^b	End Date ^b	Deposition SO ₄ ²⁻ [kg km ⁻²] ± 1σ	Start Date ^b	End Date ^b	Deposition SO ₄ ²⁻ [kg km ⁻²] ± 1σ
Pinatubo, Indonesia	1991.5	1993.5	25.4 ± 2.8	1991.7	1992.2	37.2 ± 9.2
Cerro Hudson, Chile						
Agung, Indonesia	1963.6	1965.6	16.5 ± 2.8	1963.9	1964.4	7.2 ± 7.6
Bezimianny, Kamchatka				1957.0	1958.5	8.8 ± 11.2
Hekla, Iceland				1946.8	1948.3	5.2 ± 8.5
Raikoike, Kuril Islands				1924.9	1925.4	5.7 ± 5.9
Katla, Iceland				1918.0	1920.3	5.9 ± 2.5
Katmai, Alaska				1912.8	1914.7	27.6 ± 6.1
Ksudach, Kamchatka				1908.0	1909.6	8.6 ± 5.8
St. Maria, Guatemala	1902.9	1904.3	5.4 ± 1.5			
Tarawera, New Zealand	1886.5	1887.6	5.9 ± 1.5			
Krakatoa, Indonesia	1884.0	1886.4	11.2 ± 2.6	1883.6	1886.3	18.5 ± 3.6
Grímsvötn, Iceland				1872.6	1873.5	6.2 ± 2.3
Makian, Indonesia	1862.6	1864.6	7.1 ± 2.3	1862.0	1863.7	19.3 ± 3.8
Shiveluch, Kamchatka				1856.2	1856.7	7.4 ± 2.2
Usu, Japan				1853.4	1853.9	6.5 ± 2.2
Cosiguina, Nicaragua	1834.7	1838.2	15.1 ± 2.5	1835.7	1837.6	13.1 ± 3.0
Babuyan, Philippines	1831.7	1833.2	6.9 ± 2.4	1831.4	1833.7	21.9 ± 3.0
Galunggung, Indonesia				1822.8	1823.9	10.8 ± 1.4
Tambora, Indonesia	1815.4	1818.4	88.6 ± 2.2	1815.6	1817.6	39.0 ± 2.4
Unknown	1809.4	1812.1	33.8 ± 1.8	1809.7	1811.2	30.6 ± 2.0
Grímsvötn (Laki), Iceland				1782.8	1784.5	178.6 ± 4.3
Hekla, Iceland				1766.4	1767.5	13.8 ± 2.5
Unknown	1762.1	1763.4	7.1 ± 2.1	1761.8	1763.3	12.7 ± 3.2
Katla, Iceland				1755.3	1756.6	7.9 ± 2.6
Tarumai, Japan				1739.0	1740.6	24.6 ± 3.0
Lanzarote ?				1729.2	1732.5	27.0 ± 3.7
Fuji, Japan				1707.8	1709.4	5.8 ± 1.4
Unknown	1694.6	1697.4	38.7 ± 2.8	1695.0	1696.3	20.0 ± 2.3
Gamkonora, Indonesia	1673.7	1676.0	11.5 ± 3.6	1674.2	1676.2	6.4 ± 3.1
Tarumai, Japan				1667.6	1668.5	25.6 ± 3.0
Unknown	1662.5	1664.0	5.7 ± 3.2			
Unknown				1654.4	1655.1	13.0 ± 2.3
Shiveluch, Kamchatka ?				1646.2	1646.9	21.5 ± 2.4
Parker Peak, Philippines	1641.6	1643.7	12.4 ± 2.3	1641.1	1643.3	46.8 ± 4.2
Kelut, Indonesia						
Unknown				1637.0	1637.5	12.1 ± 2.5
Unknown	1620.8	1623.0	17.8 ± 2.1			
Huaynaputina, Peru	1600.4	1603.3	24.0 ± 4.0	1601.1	1603.1	30.4 ± 3.6
Ruiz, Colombia	1594.7	1597.5	32.8 ± 5.1	1595.1	1597.4	18.5 ± 4.7
Unknown	1590.8	1592.3	6.0 ± 2.6			
Colima, Mexico	1585.8	1587.0	8.9 ± 3.1	1584.8	1586.4	24.7 ± 3.2
Billy Mitchell, S-Pacific ?				1567.4	1568.4	6.6 ± 2.2
Katla, Iceland ?				1554.0	1554.6	9.8 ± 1.6
Augustine, Alaska ?				1537.2	1538.3	6.7 ± 2.0
Hekla, Iceland				1512.4	1513.0	19.8 ± 2.1
Unknown	1504.9	1508.1	8.0 ± 2.4			
Katla, Iceland				1502.5	1503.1	6.9 ± 2.0
Bárdarbunga, Iceland				1476.8	1478.2	14.8 ± 3.2
Sakura Jima, Japan				1470.3	1470.8	10.1 ± 2.4
“Kuwae” 1458/1459	1458.4	1461.4	103.8 ± 4.1	1459.1	1461.4	36.6 ± 3.6
Unknown 1452/1453	1453.4	1454.9	8.0 ± 2.7	1453.1	1454.2	21.6 ± 2.8
Unknown	1447.6	1449.2	7.5 ± 2.8			
Unknown	1389.8	1391.2	3.5 ± 3.7	1389.1	1390.0	9.7 ± 2.3
Unknown	1377.8	1379.7	7.2 ± 1.8			
Unknown	1344.5	1348.1	20.6 ± 3.3	1344.9	1347.3	22.4 ± 3.6
Unknown				1340.9	1341.7	6.8 ± 2.2
Unknown	1336.3	1337.6	5.0 ± 1.6			
Unknown	1330.6	1332.1	9.0 ± 2.4	1328.9	1332.1	32.1 ± 5.4
Unknown	1306.3	1307.1	5.7 ± 1.7			
Unknown	1294.5	1295.9	9.8 ± 2.4			
Unknown	1290.4	1292.2	6.2 ± 2.2			
Unknown	1285.6	1288.2	20.8 ± 2.8	1286.8	1289.6	28.7 ± 2.9
Unknown	1276.5	1278.7	31.9 ± 2.9			
Unknown	1269.5	1271.4	20.1 ± 2.6			
Unknown	1257.9	1261.1	79.7 ± 2.8	1258.2	1260.6	82.1 ± 2.2
Unknown	1241.3	1242.4	12.3 ± 2.3			

(Continues)

Table 1. (continued)

Volcano, Region	WDC06A			NEEM S1		
	Start Date ^b	End Date ^b	Deposition SO ₄ ²⁻ [kg km ⁻²] ± 1σ	Start Date ^b	End Date ^b	Deposition SO ₄ ²⁻ [kg km ⁻²] ± 1σ
Unknown	1229.6	1233.1	35.8 ± 2.9	1229.3	1232.5	51.4 ± 4.9
Unknown				1220.1	1220.6	8.2 ± 2.4
Unknown				1208.4	1214.6	36.5 ± 5.8
Unknown				1196.9	1198.5	11.1 ± 3.5
Unknown	1189.4	1191.1	14.5 ± 2.8	1188.6	1189.7	15.2 ± 3.1
Unknown				1179.6	1180.7	42.7 ± 2.6
Unknown	1169.7	1171.9	26.9 ± 3.1	1168.1	1170.2	37.4 ± 2.5
Unknown	1149.1	1150.1	5.5 ± 1.9			
Unknown				1124.0	1125.5	18.0 ± 2.6
Unknown				1110.7	1111.5	5.9 ± 4.1 ^c
Hekla, Iceland	1107.0	1108.5	8.5 ± 2.6	1104.9	1108.6	48.9 ± 4.6
Unknown				1063.8	1064.7	5.1 ± 2.4
Unknown				1053.9	1054.9	5.4 ± 2.3
Unknown				1046.6	1048.3	5.5 ± 3.0
Unknown	1036.4	1038.1	15.4 ± 2.9			
Unknown				1024.1	1025.9	21.9 ± 2.6
Unknown				1017.4	1019.0	13.9 ± 3.5
Unknown	997.5	999.1	5.2 ± 3.1	997.0	998.2	9.1 ± 2.5
Unknown				993.0	993.6	5.7 ± 2.4
Unknown	972.6	976.2	13.9 ± 3.3	976.1	976.6	17.3 ± 2.6
Unknown				970.9	973.6	20.5 ± 4.6
Unknown				964.1	965.3	11.9 ± 2.8
Unknown	957.2	959.1	18.9 ± 2.7			
Unknown				947.3	947.9	8.4 ± 1.9
Unknown				939.8	941.4	13.3 ± 3.1
Eldgjá, Iceland				933.3	934.9	102.5 ± 3.5
Unknown	925.4	926.0	8.7 ± 2.3	922.1	923.1	8.5 ± 2.9
Unknown	913.0	915.9	9.9 ± 2.9	910.3	914.2	23.8 ± 5.2
Unknown				897.0	898.3	26.3 ± 3.3
Unknown	895.7	896.8	11.0 ± 2.3	893.1	893.6	6.7 ± 2.5
Unknown	877.5	878.4	9.7 ± 2.2			
Bárdarbunga, Iceland ?				870.7	874.1	38.6 ± 5.5
Unknown				866.0	866.4	11.6 ± 2.6
Unknown	853.4	855.2	7.6 ± 2.3	852.9	853.6	8.4 ± 3.6
Unknown				847.0	849.2	20.6 ± 3.9
Unknown				840.5	840.8	9.1 ± 2.5
Unknown				835.1	835.5	7.4 ± 2.8
Unknown				816.1	817.3	44.4 ± 6.9
Unknown	811.7	813.4	7.4 ± 3.4	811.4	815.1	66.8 ± 6.2
Unknown				793.0	795.2	23.5 ± 4.5
Unknown				775.2	776.4	21.7 ± 3.5
Unknown				755.9	756.9	17.6 ± 2.9
Unknown	747.5	749.1	8.2 ± 1.7	748.1	750.8	31.1 ± 6.1
Unknown	741.8	743.9	12.8 ± 2.6	742.3	746.2	63.2 ± 6.8
Unknown	738.0	741.0	14.4 ± 3.2			
Unknown	733.8	736.1	6.3 ± 3.1			
Unknown				723.5	724.2	5.8 ± 2.4
Unknown	717.9	719.3	7.3 ± 1.9			
Unknown	689.7	691.3	10.0 ± 3.9	690.4	691.2	3.9 ± 1.8
Unknown				686.4	687.2	9.2 ± 2.0
Unknown	676.5	678.9	31.6 ± 3.1	678.0	681.4	19.6 ± 3.9
Unknown	674.1	676.1	36.9 ± 3.0	674.4	676.3	45.5 ± 2.8
Unknown				630.1	630.6	5.7 ± 1.4
Unknown				624.8	626.2	14.3 ± 2.0
Unknown				619.1	622.3	89.9 ± 3.2
Unknown	607.5	608.1	10.1 ± 4.3			
Unknown	579.7	581.2	7.5 ± 2.2	582.3	582.8	6.1 ± 2.0
Unknown	565.8	569.0	54.8 ± 3.9	567.0	569.0	33.7 ± 2.5
Unknown				539.5	541.0	8.7 ± 5.3 ^c
Unknown	531.2	534.6	33.1 ± 4.9	532.5	535.0	66.1 ± 4.0
Unknown	528.7	530.2	8.3 ± 3.5	529.8	531.5	101.5 ± 5.8 ^c
Unknown				515.5	517.5	30.4 ± 2.6 ^c
Unknown				495.5	496.4	17.8 ± 3.4
Unknown	485.4	487.3	19.6 ± 2.8			
Unknown	478.6	480.0	6.5 ± 1.9			
Unknown				463.2	464.1	8.4 ± 2.1
Unknown				461.0	461.5	16.7 ± 2.2

(Continues)

Table 1. (continued)

Volcano, Region	WDC06A			NEEM S1		
	Start Date ^b	End Date ^b	Deposition SO ₄ ²⁻ [kg km ⁻²] ± 1σ	Start Date ^b	End Date ^b	Deposition SO ₄ ²⁻ [kg km ⁻²] ± 1σ
Unknown				449.5	450.9	11.6 ± 2.3
Unknown	438.4	439.9	10.0 ± 3.0			
Unknown	426.4	428.8	44.5 ± 2.6	425.4	426.5	23.7 ± 2.7
Unknown				418.8	419.6	12.0 ± 2.8
Unknown				416.1	417.3	8.0 ± 2.0
Unknown				411.2	411.7	8.7 ± 1.9
Unknown				404.1	404.8	11.7 ± 2.6
Unknown	385.8	388.2	8.3 ± 2.9	385.1	385.6	9.8 ± 1.7
Unknown	374.4	375.0	12.5 ± 2.0			
Unknown	371.5	372.7	10.1 ± 3.5			
Unknown				361.4	362.4	12.8 ± 2.3
Unknown				358.3	359.0	14.4 ± 1.7
Unknown	352.7	353.2	7.7 ± 1.7	350.3	351.0	6.8 ± 1.3
Unknown	345.5	346.6	5.5 ± 2.9			
Unknown				340.2	340.7	12.3 ± 1.3
Unknown	336.8	339.2	14.4 ± 3.6	337.9	338.5	4.0 ± 1.4
Unknown	323.7	327.2	10.9 ± 4.2			
Unknown	298.5	300.1	20.5 ± 4.3	297.7	299.2	10.9 ± 3.7
Unknown				294.9	295.5	10.3 ± 2.5
Unknown				275.3	277.9	42.0 ± 5.2
Unknown	261.1	263.2	17.4 ± 2.8	258.1	260.6	66.5 ± 3.7
Taupo, New Zealand	231.8	235.2	13.2 ± 3.0	230.8	233.7	14.5 ± 4.3
Unknown				221.3	221.8	15.4 ± 2.7
Unknown	212.8	214.1	8.6 ± 3.4	213.2	213.7	7.5 ± 2.7
Unknown	199.4	201.1	30.1 ± 3.6			
Unknown				185.9	187.0	5.3 ± 1.8
Unknown				164.7	166.3	8.8 ± 2.9
Unknown	163.4	165.1	25.6 ± 3.2	161.0	162.7	39.1 ± 3.3
Unknown				153.1	154.6	17.0 ± 3.0
Unknown	136.3	138.2	10.7 ± 3.3			
Unknown	117.6	119.3	11.4 ± 3.3			
Unknown	114.6	116.2	9.1 ± 3.1			
Unknown				107.0	108.4	17.7 ± 2.9
Unknown	98.4	99.0	7.4 ± 1.6			
Unknown	87.7	88.3	6.7 ± 2.9			
Vesuvius, Italy				79.1	81.0	83.1 ± 4.4
Unknown	75.5	76.7	10.8 ± 2.7			
Unknown	23.1	24.2	6.8 ± 1.9			
Unknown	-3.5	-2.9	5.7 ± 1.8			
Unknown	-13.5	-12.3	9.0 ± 2.6			
Unknown	-27.7	-25.4	10.1 ± 2.4			
Unknown	-54.6	-52.3	26.2 ± 3.3			
Unknown	-93.9	-91.8	9.3 ± 2.6			
Unknown	-109.3	-105.7	24.5 ± 3.8			
Unknown	-147.8	-145.1	15.0 ± 2.1			
Unknown	-160.5	-157.9	8.4 ± 2.6			
Unknown	-183.3	-180.7	16.4 ± 3.1			
Unknown	-203.5	-202.2	5.6 ± 2.2			
Unknown	-222.7	-220.9	23.6 ± 2.7			
Unknown	-258.1	-257.2	16.1 ± 2.0			
Unknown	-337.8	-335.2	24.4 ± 4.3			
Unknown	-371.5	-369.0	16.9 ± 3.0			
Unknown	-388.8	-388.1	6.3 ± 1.9			
Unknown	-405.4	-403.1	13.1 ± 2.4			

^aOnly eruptions with >5 kg km⁻² volcanic sulfate deposition are shown. Bipolar signals are indicated in bold letters.

^bThe error in the estimate of the fraction of the year is ±0.25 (equivalent to 3 months) based on intra-annual variability in snow accumulation

^cSulfate fluxes calculated using fast ion chromatography SO₄²⁻ data from the main NEEM ice core

one hemisphere could as well be from a tropical eruption and the absence of a signal in the other hemisphere a result of the individual geographical deposition pattern. Besides additional sulfur isotope and tephra studies, a large number of individual volcanic records from both hemispheres from ice cores or alternative volcano proxy series (e.g., historic accounts), may help to reconstruct the major tropical eruptions of the past.

4. Discussion

4.1. “Kuwae” (1452/1458)

[46] In a comprehensive analysis, the greatest volcanic sulfate event of the last 700 years was associated with the eruption of the Kuwae volcano in Vanuatu (16.83S, 168.54W) and an eruption date of late 1452 or early 1453 was ascribed to the event [Gao *et al.*, 2006]. In the following,

Table 2. Comparison of Volcanic Sulfate Flux Between Annual Layer Counted Ice Core Records From Antarctica (a) and Greenland (b)

a:

Reference	This Study	This Study	Cole Dai 2011 ^a	Plummer 2012 ^b	Traufetter 2004 ^c	Ferris 2011 ^d	Gao 2006/07 ^e
Volcano	WAIS WDC06A SO ₄ ²⁻ (kg km ⁻²)	WAIS WDC05Q SO ₄ ²⁻ (kg km ⁻²)	WAIS WDC05Q SO ₄ ²⁻ (kg km ⁻²)	Law Dome DSS SO ₄ ²⁻ (kg km ⁻²)	DML B32 SO ₄ ²⁻ (kg km ⁻²)	South Pole SP04 SO ₄ ²⁻ (kg km ⁻²)	Antarctic Composite ^f SO ₄ ²⁻ (kg km ⁻²)
Krakatao 1883	11.2	14.2	no data reported	17.2	9.7	12.9	12.1 ± 5.9
Tambora 1815	88.6	92.1	81.0	58.4	32.5	26.3	56.7 ± 32.8
Unknown 1809	33.8	48.4	41.0	25.2	15.4	23.1	25.1 ± 13.3
Kuwae 1458	103.8	no data	no data	108.6	47.0	75.2	93.0 ± 35.5
Unknown 1258	79.7	no data	no data	103.3	74.3	99.3	112 ^g
Unknown 674	36.9	no data	no data	30.5	35.9	38.4	no data reported
Unknown 566	54.8	no data	no data	25.7	37.5	no signal	no data reported
Unknown 532	33.1	no data	no data	37.7	29.2	41.9	no data reported
Unknown 426	44.5	no data	no data	64.4	16.2	14.7	no data reported

b:

Reference	This Study	This Study	Plummer 2012 ^b	Gao 2006/07 ^e
Volcano	NEEM S1	Humboldt	NGRIP	Greenland Composite ⁱ
Krakatao 1883	18.5	12.6	15.4	14.0 ± 7.4
Tambora 1815	39.0	35.4	40.3	49.5 ± 24.8
Unknown 1809	30.6	>6.1 ^h	38.6	25.9 ± 15.2
Kuwae 1458	36.6	42.2	41.4	no data reported
Unknown 1258	82.1	70.0	98.6	146 ^j
Unknown 674	45.5	no data	31.1	no data reported
Unknown 566	33.7	no data	42.9	no data reported
Unknown 532	66.1	no data	56.2	no data reported
Unknown 426	23.7	no data	17.5	no data reported

^aCole-Dai *et al.*, [2009]^bPlummer *et al.*, [2012]^cTraufetter *et al.*, [2004]^dFerris *et al.*, [2011]^eGao *et al.*, [2006, 2007]^fmean sulfate flux and standard deviation from 17 Antarctic ice core volcano records. See details in Gao *et al.*, [2006]^gthe original average deposition from the 5 ice core records containing the event has been multiplied by 1.27 to account for the spatial variability in sulfate deposition. The correction factor was calculated by comparing the average deposition of those 5 records to the average deposition of all 17 Antarctic ice core records. See details in Gao *et al.*, [2007]^hsignal is partly missingⁱmean sulfate flux and standard deviation from 7 Northern Hemisphere (Greenland, Alaska) ice core volcano records. See details in Gao *et al.*, [2006]^jthe original average deposition from the 3 ice core records containing the event has been multiplied by 1.13 to account for the spatial variability in sulfate deposition. The correction factor was calculated by comparing the average deposition of those 3 records to the average deposition of all 7 Northern Hemisphere ice core records. See details in Gao *et al.*, [2007]

we will summarize the lines of evidence that led to this attribution and contrast it in light of new evidence from the WDC06A and NEEM S1 ice cores.

[47] The first evidence of a large tropical eruption came from an acidity signal recorded in an ice core from the South Pole [Delmas *et al.*, 1992]. An age estimate of 1450 ± 10 was given for the sulfate signal that lasted for 3 years. A global extent of the sulfate deposition was deduced from ice cores of Crete and Dye (Greenland) and Byrd (Antarctica) with lower

dating uncertainties and an average deposition age estimate of 1460 [Langway, Osada, Clausen, Hammer, and Shoji, 1995]. The sulfate signal from these ice cores was attributed to the massive eruption of the Kuwae volcano in the South Pacific that, based on independent geological evidence, took place in the mid-15th century [Eissen, Monzier, and Robin, 1994; Monzier, Robin, and Eissen, 1994]. Various historical records and frost rings in tree ring records, summarized by Pang (1993), indicate climate effects for the year 1453 that

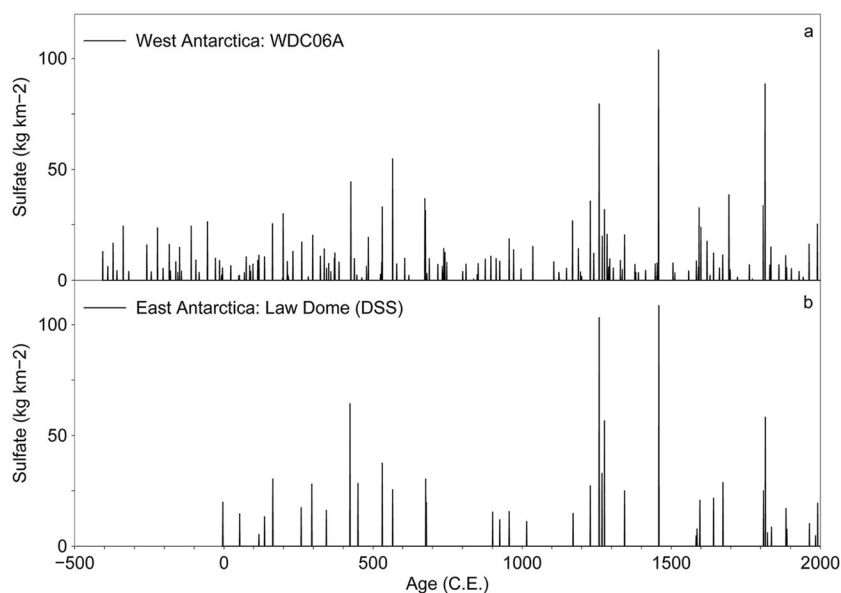


Figure 5. Comparison of the volcanic sulfate flux record derived from (a) the WDC06A volcano record of West Antarctica (b) and the Law Dome DSS volcano record [Plummer *et al.*, 2012] from East Antarctica during the last 2400 years.

typically follow large stratospheric eruptions. A major cooling event detected in 1453 from a larger network of temperature-sensitive tree ring density chronologies from the circumpolar region of the Northern Hemisphere seemed to confirm the eruption date of 1452 and the global extent of its climate effects [Briffa, Jones, Schweingruber, and Osborn, 1998]. After the eruption date was seemingly confirmed, the prominent sulfate signal was used widely as a fixed time marker for dating Antarctic ice cores [Cole-Dai, Mosley-Thompson, Wight, and Thompson, 2000; Ferris *et al.*, 2011; Stenni *et al.*, 2002]. Evidence from the northern hemispheric ice

cores seems less clear, however. Specifically, several of the Greenland ice cores show two signals: one in the mid-1450s and another at the beginning of the 1460s [Gao *et al.*, 2006]. NorthGRIP, the ice core site with the lowest dating uncertainty (data based on the GICC05 timescale with an estimated counting error of 0.25% for the Holocene), has two volcanic sulfate signals: in the year 1453 and in 1459 [Gao *et al.*, 2006]. The GISP2 record shows only one major signal from 1459-1462 [Zielinski, 1995].

[48] The new NEEM S1 record agrees with NorthGRIP in showing two major volcanic signals (Figure 6). A first

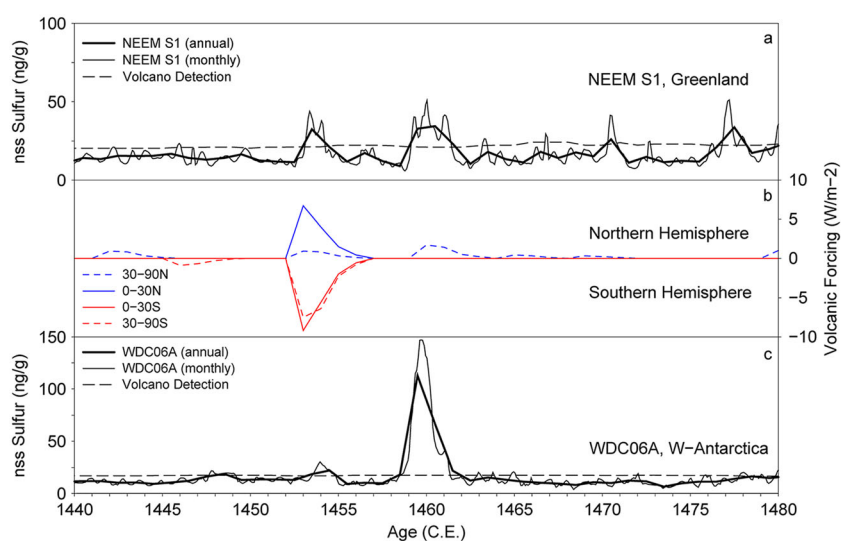


Figure 6. Annually (bold lines) and monthly (thin lines) averaged nssS concentration records from (a) NEEM S1 and (c) WDC06A between 1440 and 1480 C.E. showing volcanic signals previously linked to the eruption of Kuwae, Vanuatu with volcano detection threshold (dashed lines) as described in figure 4. A volcanic forcing series (b) based on previous dating attempts shows estimates of radiative forcing separately for high and low latitudes of both hemispheres [Hegerl *et al.*, 2007]. Northern hemispheric forcing is displayed on an inverse scale.

eruption led to deposition of 22 kg km^{-2} sulfate during 2 years starting in 1453. It was followed by a larger, second event starting in 1459 that lasted for 3 years and deposited 37 kg km^{-2} sulfate. The dating accuracy for both events is very high (± 1 a) due to the proximity of the volcanic time marker from the Bárðarbunga eruption taking place in Iceland in 1477.

[49] In the new WAIS Divide ice core, the largest sulfate signal of the last 2400 years was between 1458 and 1461 CE (Figure 6) The magnitude is consistent with most of Antarctic ice cores [Gao *et al.*, 2006]. With a conservative interpretation uncertainty of 1% for the annual layer count, the absolute age uncertainty for this event in WDC06A is ± 2 a (140 annual layers identified since the last volcanic tie point of Huaynaputina (19 February 1600; Peru). This is less than the reported dating uncertainty of the few unmatched sulfate records used in the study that placed the date of the eruption in 1452/53 [Gao *et al.*, 2006]. The ages and uncertainties of the beginning of the event in the original references are 1454 ± 3 for Siple Station [Cole-Dai, Mosley-Thompson, and Thompson, 1997], 1453 ± 5 for Dronning Maud Land B32 [Traufetter *et al.*, 2004], 1456 ± 3 for South Pole SP01 [Budner and Cole-Dai, 2003], and 1459 ± 1 for Law Dome DSS [Palmer *et al.*, 2001]. It is surprising that the date from the high accumulation ice core of Law Dome (0.7 m/a ice equivalent) recently confirmed to be 1458 ± 1 [Plummer *et al.*, 2012] was outnumbered by a few uncertain dates from low accumulation ice core sites in Antarctica in the interpretation by Gao *et al.* (2006). Their main argument to devalue the accuracy of the Law Dome timescale was that annual layers might be missing at conjunctions of the three ice cores used for the composited Law Dome record [Gao *et al.*, 2006]. These conjunctions, however, were at 1888 and 1841; and many well constrained time markers (e.g., Tambora, 1815; Gamkonora, 1673; Huaynaputina 1600) are identified with the correct ages below, suggesting no loss of annual layers during formulation of the timescale [Palmer *et al.*, 2001].

[50] Taking evidence from the five high precision dated ice cores of Law Dome [Palmer *et al.*, 2001; Plummer *et al.*, 2012] and WAIS Divide (this study) from Antarctica as well as NEEM (this study), NorthGRIP [Gao *et al.*, 2006; Plummer *et al.*, 2012], and GISP2 [Zielinski, 1995] from Greenland suggests that the major stratospheric eruption attributed to the Kuwae volcano took place probably in 1457 or 1458, 5 to 6 years later than was assumed. This is in agreement with evidence from temperature-sensitive tree ring records showing pronounced growth reduction between 1458 and 1462 [Salzer and Hughes, 2007].

[51] Furthermore, the new high-resolution volcanic record from WAIS Divide shows evidence of a second volcanic event in 1453 (Figure 6), contradicting the assumption that only one major eruption took place in the mid-15th century [Gao *et al.*, 2006]. A recent ice core record from the South Pole (SP04) confirms a second signal (SP04-15, volcanic flux: 4 kg km^{-2} sulfate) preceding the main event by 5 years [Ferris *et al.*, 2011]. A sulfate flux of only 8 kg km^{-2} in WDC06A and a short time lag compared to the sulfate signal in the NEEM S1 record suggests a tropical eruption source in the Northern Hemisphere. The strong response in maximum-density tree ring records in Scandinavia [Buntgen *et al.*, 2011a; Esper, Buntgen, Timonen, and Frank, 2012]

and in the circumpolar tree ring networks [Briffa *et al.*, 1998; Jones *et al.*, 1995] as well as historical accounts in Europe and China [Pang, 1993] suggest a volcanic eruption in late 1452/early 1453.

[52] The overall evidence of all available ice core and tree ring data to date indicates that two tropical eruptions took place, the first probably occurred in 1452 explaining the described phenomena from historical accounts from Europe and China and leading to widespread reduced tree growth in 1453. Since the sulfate flux was stronger in Greenland than Antarctica, we suggest a source volcano in the low latitudes of the Northern Hemisphere. A second strong eruption probably took place in 1457/1458 explaining the large ice core sulfate signals starting at 1458 in Antarctica and 1459 in Greenland. Climatic effects of this eruption that probably occurred in the low latitudes of the Southern Hemisphere can be detected in temperature-sensitive tree ring series in Europe and North America. While volcanic tracers and tree ring response indicated two major stratospheric eruptions during this time, with the later one being one of the largest eruptions during the last 2000 years, additional analysis of sulfur isotopes [Savarino *et al.*, 2003] from these events could bring additional confidence to this interpretation.

4.2. Taupo Eruption (232)

[53] The most violent eruption of the last 5000 years took place in the Taupo Volcanic Zone of North Island, New Zealand. It is believed that the eruption column reached as high as 50 km and that a large amount of tephra, ash, and sulfate aerosols was injected into the stratosphere and displaced in both hemispheres [Wilson, 1993].

[54] Based on historical accounts from China and Rome, the eruption was initially placed in the year 186 [Wilson, Ambraseys, Bradley, and Walker, 1980] and was seemingly confirmed by a sulfate spike in the GISP2 record of Greenland in 181 ± 2 [Zielinski *et al.*, 1994]. Matching a ^{14}C chronology from trees affected by the eruption to the radiocarbon calibration curve by Stuiver and Becker (1993), however, yielded an eruption date of 232 ± 15 [Sparks *et al.*, 1995]. With an alternative age estimate for seemingly the same event available, it was for future investigators to choose the correct age. Many ice core records followed the link to GISP2 in attributing sulfate peaks at the end of the 2nd century to the ice core/historical account date of 186 [Cole-Dai *et al.*, 2000; Ferris *et al.*, 2011; Traufetter *et al.*, 2004]. The date of 186 also has been used as a fixed tie-point in establishing an ice core chronology in East Antarctica [Ren *et al.*, 2010]. Alternatively, a global tsunami probably caused by the violent eruption of Taupo was tentatively dated to c. 200 CE to bypass the obvious age offset to the younger, tree ring derived ages [Lowe and de Lange, 2000]. Recently, the radiocarbon-based age was confirmed by wiggle matching 25 high-precision ^{14}C dates of buried trees against a regional radiocarbon calibration data set [Hogg, Lowe, Palmer, Boswijk, and Ramsey, 2012]. The revised date for the violent Taupo eruption is thereafter 232 ± 5 .

[55] Figure 7 displays the sulfur records for WDC06A and NEEM S1 between 150 and 270. Assuming that the large signals at NEEM in 161 and 258 and at WAIS Divide in 163 and 261 result from tropical eruptions implies that the two independent timescales agree within 2–3 years for this

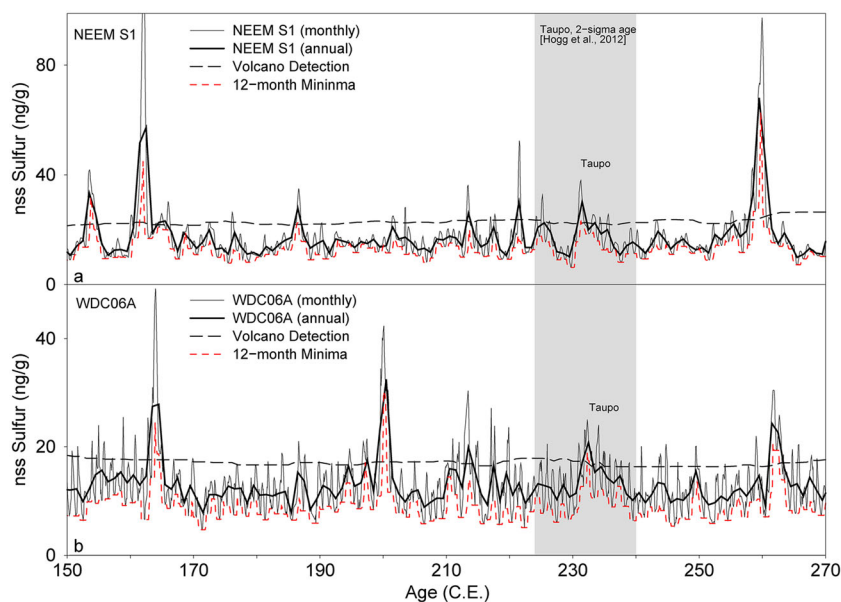


Figure 7. Annually (bold lines) and monthly (thin lines) averaged nssS concentration records from (a) WDC06A and (b) NEEM S1, between 150 and 270 C.E. showing volcanic signals related to the eruption of Taupo, New Zealand with an independent, calibrated (2-sigma) ^{14}C age estimate of 224–240 C.E. [Hogg *et al.*, 2012] with volcano detection threshold (dashed lines) and a 12 month running minimum (red dashed lines).

time window. Since the volcanic tie-point of the Vesuvian eruption carrying a calendar age is close in the NEEM S1 timescale, absolute dating uncertainty is as low as ± 2 years for NEEM S1, which could be adapted for WDC06A given the close match of these timescales. In between those two pairs of signals, there are several volcanic signals recorded in the ice. For NEEM S1, there were volcanic events in 186, 213, 221, and 231. WDC06A had signals in 199, 213, and 232. Sulfate peaks from Antarctic ice cores that claim to be from an eruption in 186 [e.g., Traufetter *et al.*, 2004; Ferris *et al.*, 2011] are shifted by up to ± 20 years relative to their original timescale after synchronizing to the more accurate WAIS volcano record (see Figure 2). No volcano record from Antarctica, including WAIS and also the new record from Law Dome [Plummer *et al.*, 2012], contains a volcanic signal around the year 186. This suggests that the event reported by Zielinski *et al.* (1994) with climate effects described in 186 is probably from an eruption in the Northern Hemisphere.

[56] The signals in 231/232 are most likely representing the Taupo eruption and confirming the new high-precision radiocarbon date of 232 ± 5 . The characteristic evolution of the signal at around 232 in both ice cores, highlighted through the high-resolution measurements (see Figure 7), give confidence in addressing the same event in both hemispheres. While, during this event, the maximum values of sulfur in each annual cycle were only moderately enhanced compared to other volcanic signals, the annual minimum values are above the natural background for up to 7 consecutive years. This suggests a moderate but long-lasting flux of volcanic sulfur which might be an effect of the high eruption column and subsequent size-dependent fallout of volcanic aerosols from the stratosphere [Wilson and Walker, 1985]. Sulfate flux for the event was 15 kg km^{-2} (NEEM S1) and 13 kg km^{-2} (WDC06A). To date, no tephra from this eruption

has been reported for the various ice cores in Greenland and Antarctica that could verify assignment of the reported ice core signals to the Taupo eruption.

4.3. Volcanic Forcing and Tree Ring Response

[57] In addition to the direct chemical imprint measured in ice cores, large volcanic eruptions can leave fingerprints in the growth of trees as these events lead to significant summer cooling in the year following the eruption [Briffa *et al.*, 1998; Jones *et al.*, 1995]. This well-known relationship is illustrated in Figure 8.

[58] By contrasting climate model simulations and tree ring reconstructions following the three large eruption pulses of 1258/1259, 1452/1453, and 1809+1815, a damping and shifting of the tree ring cooling response of major volcanic eruptions has been identified [Mann, Fuentes, and Rutherford, 2012]. Simulations with a tree growth model suggest that in years after large eruptions, the growing season might be too short to build a tree ring, thus leading to chronological errors that would accumulate back in time [Mann *et al.*, 2012]. While this hypothesis has been rejected on the basis of the applied tree growth model and empirical evidence [Anshukaitis *et al.*, 2012], evidence from our new ice core records suggests that these results are additionally biased by chronological errors in the volcanic forcing index used in their simulations. While the index by Gao *et al.* (2008) erroneously assumes strong volcanic forcing by placing the “Kuwaē” eruption in 1453, we suggested a stronger volcanic forcing in 1458/1459 instead, thus explaining a time shift in tree ring response. Figure 9 displays the tree ring response expressed in a climate sensitive ring width chronology from upper tree line *Bristlecone Pines* in the western United States [Salzer and Hughes, 2007] and in a climate sensitive maximum latewood density chronology from a boreal tree ring network in Scandinavia [Esper *et al.*,

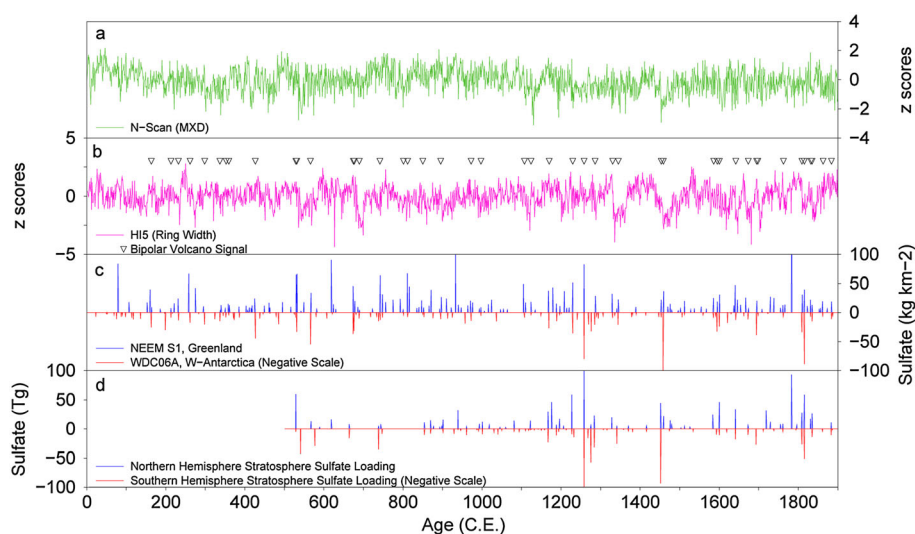


Figure 8. (a) Summer temperature (JJA) reconstruction from Scandinavia based on maximum latewood density (MXD) records from *Pinus sylvestris* [Esper *et al.*, 2012] normalized to the time period 1–2000 C.E. (green), (b) Tree ring index from the upper tree line bristlecone pine HI5 chronology (*Pinus longaeva* and *Pinus aristata*), Great Basin, USA. [Salzer and Hughes, 2007] normalized to the time period 1–2000 C.E. (purple) with triangles indicating bipolar volcano signals from the WDC06A/NEEM S1 volcano record on the WDC06A timescale, (c) Bipolar volcanic ice core record with sulfate flux from NEEM S1 (blue) and WDC06A (red, negative scale). (d) Volcanic forcing index from Gao *et al.* (2008) separately for the Northern Hemisphere (blue) and Southern Hemisphere (red, negative scale).

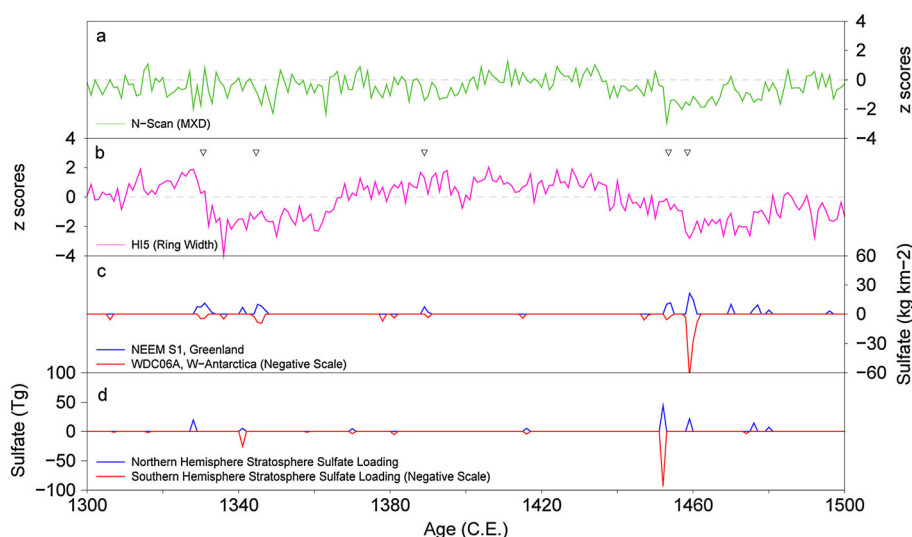


Figure 9. Detailed record of tree ring response to volcanic forcing between 1300 and 1500 C.E. (a/b). See figure 8 for additional information on the individual time-series. (c) Bipolar volcanic ice core record with sulfate flux from NEEM S1 (blue) and WDC06A (red, negative scale); other than in figure 8, volcanic fluxes of WDC06A and NEEM S1 are presented on an annual basis instead of summing the flux of individual events. (d) Volcanic forcing index from Gao *et al.* (2008) separately for the Northern Hemisphere (blue) and Southern Hemisphere (red, negative scale).

2012] between 1300 and 1500. Following the tropical eruptions in 1452/1453, Scandinavian trees indicate cooling with decreased maximum densities lasting for a decade. The tree rings in western United States show a cooling response after 1458 only, but with reduced tree ring widths lasting for almost 20 years. A similar strong response was observed

220 years earlier after a large tropical eruption in 1330 and consecutive eruptions in 1336, 1340, 1344. This might be explained by a cumulative effect of multiple closely spaced eruptions. Closely spaced volcanic signals appear frequently in our bi-hemispheric ice core record during the last 2000 years and seem to strongly affect tree growth (Figure 9).

[59] We investigated tree ring response to the WDC06A/NEEM S1 ice core volcanic record by contrasting single events (defined as only one eruption within 9 years: 1170, 1229, 1258, 1276, 1285) with double events (two large eruptions within less than 8 years: 1330/1336, 1452/1458, 1595/1600, 1641/1646, 1667/1673, 1809/1815, 1831/1835) separately for both eruptions (Figure 10). We restricted our analysis to the last 1000 years and to the largest events, with a cumulative total sulfate deposition rates of $>40 \text{ kg km}^{-2}$ sulfate comparable to a stratospheric sulfate injection of 40 Tg using the calibration factor by Gao *et al.* (2007). We further excluded Icelandic eruptions (e.g., Laki, Hekla), since sulfate injection to the stratosphere and thus a climate effect is supposed to have been low [Lanciki, Cole-Dai, Thiemens, and Savarino, 2012].

[60] Maximum latewood density series from Scandinavia showed a strong summer temperature response in the year of the eruption or 1 year later, in agreement with the temperature response from climate models and observations [Fischer *et al.*, 2007; Thomas, Timmreck, Giorgetta, Graf, and Stenchikov, 2009]. Differences between a single eruption and the first and second eruption of an eruption doublet were low, suggesting no biological memory in the formation of latewood. In contrast, ring width response from the upper tree line showed smoother and longer-lasting response. In particular, after a second volcanic eruption, a sustained depression can be observed with ring widths being 1–2 standard deviations lower than before the eruption for more than 10 years. This strong and long-lasting response to a second eruption is best explained by the loss of carbohydrate

reserves after the prior eruption [Anchukaitis *et al.*, 2012]. Differences between the single events which showed no sustained depression in the ring widths and the first event of doublets which showed sustained depression probably is also explained by the preconditioning climate. While most of the doublets occurred during the Little Ice Age (LIA) with temperatures being colder and thus tree growth being more sensitive to temperature perturbations, the large volcanic single events occurred during the warmer 12th and 13th centuries before those events triggered the feedbacks that finally led into the LIA period [Miller *et al.*, 2012]. This simple comparison based on new ice core evidence clearly showed the advantage of maximum latewood density over tree ring width in capturing past temperatures. As more and longer latewood density chronologies are emerging [Buntgen *et al.*, 2011; Esper *et al.*, 2012], this will allow analysis of climate response to volcanic forcing for longer time periods than in the past, which is still strongly limited by the dating accuracy of the ice core timescales.

5. Conclusion

[61] In current practice, accuracy in estimating past volcanic forcing is limited by the dating accuracy of Antarctic ice core timescales. The WAIS Divide WDC06A ice core has provided a well-dated volcanic record as the relatively high-accumulation rates combined with a high-resolution continuous melting technique allowed for a high-accuracy timescale with seasonal resolution during the last 2400 years. At the same time, because of the large distance from the ocean, background levels

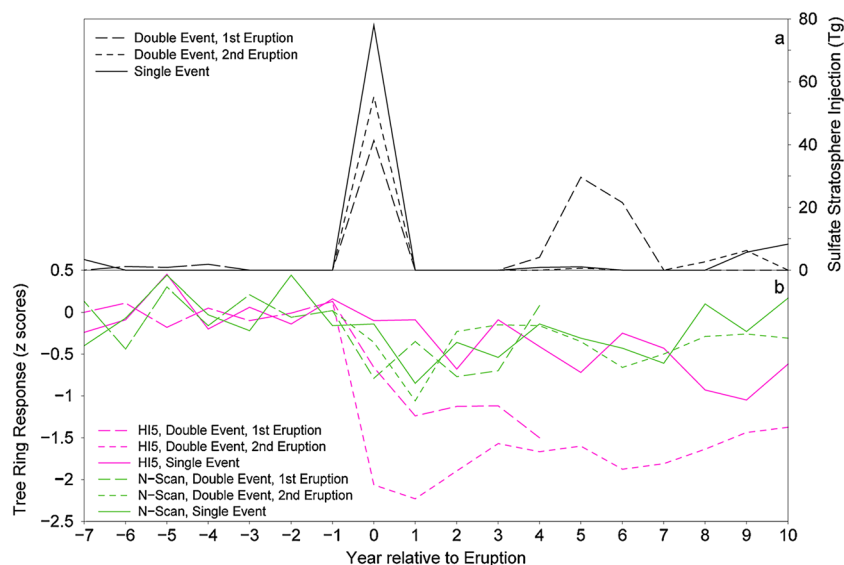


Figure 10. (a) Volcanic sulfate stratospheric injection estimated from NEEM S1 and WDC06A sulfate deposition applying calibration factors developed by Gao *et al.* (2007) – relative to the eruption year, assuming a delay time of 0.5 to 1 a between eruption and start of deposition. Only volcanic single events or series of closely spaced events during the last 1000 years exceeding 40 Tg sulfate injection were used for the analysis. Large eruptions from Iceland with little expected sulfate injection into the stratosphere (e.g., Laki 1783, Hekla 1104) are excluded. Volcanic signals are separated into three categories: “Single Events” (1170, 1229, 1258, 1276 and 1285), “Double Event 1st eruption” (1330, 1453, 1595, 1641, 1667, 1809 and 1831), and “Double Event 2nd eruption” (1336, 1458, 1600, 1646, 1673, 1815 and 1835). (b) Normalized tree ring response relative to the 7 years preceding the first volcanic eruption for Scandinavia MXD (green) and the HI5 bristlecone pine ring width index (purple), separately for the three event categories. See figure 8 for detailed information on the individual time series.

of nonvolcanic sulfate deposition are low in this core, allowing detection of more volcanic events than in previous Antarctic ice core records. We detected 20% more bi-hemispheric events which are predominantly caused by tropical volcanic eruptions and have a strong impact on global temperatures. We showed for the first time ice core signals in Greenland and Antarctica ascribed to the eruption of Taupo (232 CE), which was the strongest volcanic eruption of the last 2000 years. Both the WDC06A and NEEM S1 records showed a sharp but moderate increase in sulfur concentrations followed by a slow decline to background levels lasting 5–7 years after this event. This unusual shape might be explained by the exceptionally high eruption column releasing volcanic aerosols 50 km into the stratosphere. Our high dating precision allowed placement of the large bi-hemispheric event ascribed to the Kuwae eruption (previously thought to be 1452/1453) into the year 1458/1459. This signal is the largest volcanic event in most ice core records from Antarctica and has erroneously been used as a reference time marker in establishing ice core timescales in the past. The new age is consistent with an independent ice core timescale from Law Dome [Plummer *et al.*, 2012]. A volcanic signal detected in 1453 in both hemispheres showed that there were two tropical eruptions one in 1452/1453 and one in 1458/1459. While tree rings in Northern Europe showed a stronger response to the earlier eruption, tree rings from Western North America responded more strongly after the second eruption. These results provide evidence that the delayed and smooth response of trees to volcanic forcing that has been linked to potential chronological errors in the tree ring time series is more likely the result of chronological errors in the volcanic forcing series instead. Further, they demonstrate the danger of circular arguing by using stratigraphic volcanic time markers as tie-points that are not linked to an absolutely certain calendar date for establishing timescales. While there are good reasons to use tie-points to reduce absolute age uncertainty or in the absence of annual layers, stratigraphic links are only as accurate as the original age assignment and only if the signal matches the same event.

[62] The two new volcanic records from the WDC06A and NEEM S1 ice cores, synchronized with all available ice core records to account for spatial variability in sulfate deposition, provide a basis for improving existing time-series of volcanic forcing. Synchronized timescales from the Arctic and Antarctic will allow robust temperature reconstructions during the last 2000 years on the continental scale, a target time period in the recent climate change debate [Steig *et al.*, 2009]. Extending the WAIS Divide volcanic record—which is believed to be annually dated until >15 kyrs BP—will enable links to the various timescales from Antarctica by their volcanic signatures, thus significantly improving existing depth-age scales. Potentially, global-scale events during the last ice age can be detected in both hemispheres providing a means to link the ice ages of Greenland and Antarctica that is independent from the uncertainty inherent in the gas-age/ice-age difference, when using ice core CH₄ records for synchronizing ice cores [Pedro *et al.*, 2011].

[63] **Acknowledgments.** Support for this research was provided by grants 0538427, 0839093, and 0909541 from the NSF Office of Polar Programs. We thank the numerous students and scientists involved in the ice core collection and analysis at the Desert Research Institute and at the field locations. The authors appreciate the support of the WAIS Divide

Science Coordination Office at the Desert Research Institute of Reno Nevada for the collection and distribution of the WAIS Divide ice core and related tasks (K. Taylor, NSF Grants 0230396, 0440817, 0944348; and 0944266—University of New Hampshire). The National Science Foundation Office of Polar Programs funds the Ice Drilling Program Office and Ice Drilling Design and Operations group for coring activities; the National Ice Core Laboratory, which curated the WAIS Divide ice cores and performed core processing, is funded by the National Science Foundation; we thank Raytheon Polar Services for logistics support in Antarctica; and the 109th New York Air National Guard for airlift in Antarctica and Greenland. We also appreciate the assistance of the NEEM community for logistics, drilling, science, and other support. In particular, we thank S.-B. Hansen, T. Popp, D. Mandeno, M. Leonhardt, and A. Moy for drilling the NEEM S1 core. NEEM is directed and organized by the Center of Ice and Climate at the Niels Bohr Institute and US NSF, Office of Polar Programs. It is supported by funding agencies and institutions in Belgium (FNRS-CFB and FWO), Canada (NRCan/GSC), China (CAS), Denmark (FIST), France (IPEV, CNRS/INSU, CEA and ANR), Germany (AWI), Iceland (RannIs), Japan (NIPR), Korea (KOPRI), The Netherlands (NWO/ALW), Sweden (VR), Switzerland (SNF), United Kingdom (NERC) and the USA (US NSF, Office of Polar Programs). Matthew Salzer and Jan Esper provided tree ring data.

References

- Ambrose, S. H. (1998), Late Pleistocene human population bottlenecks, volcanic winter, and differentiation of modern humans, *J. Human Evol.*, *34*(6), 623–651.
- Anchukaitis, K. J., et al. (2012), Tree rings and volcanic cooling, *Nature Geosci.*, *5*, 836–837.
- Banta, J. R., J. R. McConnell, M. M. Frey, R. C. Bales, and K. Taylor (2008), Spatial and temporal variability in snow accumulation at the West Antarctic Ice Sheet Divide over recent centuries, *J. Geophys. Res.*, *113*, D23102, doi:10.1029/2008JD010235.
- Basile, I., J. R. Petit, S. Touron, F. E. Grousset, and N. Barkov (2001), Volcanic layers in Antarctic (Vostok) ice cores: Source identification and atmospheric implications, *J. Geophys. Res.*, *106*(D23), 31,915–31,931.
- Bigler, M., D. Wagenbach, H. Fischer, J. Kipfstuhl, H. Millar, S. Sommer, and B. Stauffer (2002), Sulphate record from a northeast Greenland ice core over the last 1200 years based on continuous flow analysis, *Ann. Glaciol.*, *35*, 250–256, doi:10.3189/172756402781817158.
- Bisiaux, M. M., R. Edwards, J. R. McConnell, M. A. J. Curran, T. D. Van Ommen, A. M. Smith, T. A. Neumann, D. R. Pasteris, J. E. Penner, and K. Taylor (2012), Changes in black carbon deposition to Antarctica from two high-resolution ice core records, 1850–2000 AD, *Atmos. Chem. Phys.*, *12*(9), 4107–4115, doi:10.5194/acp-12-4107-2012.
- Bowen, H. J. M. (1979), *Environmental Chemistry of the Elements*, 333 pp., Academic Press, London.
- Briffa, K. R., P. D. Jones, F. H. Schweingruber, and T. J. Osborn (1998), Influence of volcanic eruptions on Northern Hemisphere summer temperature over the past 600 years, *Nature*, *393*(6684), 450–455, doi:10.1038/30943.
- Budner, D., and J. H. Cole-Dai (2003), The number and magnitude of large explosive volcanic eruptions between 904 and 1865 A. D.: Quantitative evidence from a new south pole ice core, in *Volcanism and the Earth's Atmosphere*, edited by A. Robock and C. Oppenheimer, pp. 165–176, AGU, Washington, D. C.
- Buntgen, U., et al. (2011a), Causes and consequences of past and projected Scandinavian summer temperatures, 500–2100 AD, *PLoS One*, *6*(9), E25133, doi:10.1371/journal.pone.0025133.
- Buntgen, U., et al. (2011b), 2500 years of European climate variability and human susceptibility, *Science*, *331*(6017), 578–582, doi:10.1126/science.1197175.
- Castellano, E., S. Becagli, M. Hansson, M. Hutterli, J. R. Petit, M. R. Rampino, M. Severi, J. P. Steffensen, R. Traversi, and R. Udisti (2005), Holocene volcanic history as recorded in the sulfate stratigraphy of the European Project for Ice Coring in Antarctica Dome C (EDC96) ice core, *J. Geophys. Res.*, *110*, D06114, doi:10.1029/2004JD005259.
- Cole-Dai, J. (2010), Volcanoes and climate, *Wiley Interdiscip. Rev.: Clim. Change*, *1*(6), 824–839, doi:10.1002/wcc.76.
- Cole-Dai, J. H., E. Mosley-Thompson, and L. G. Thompson (1997), Annually resolved southern hemisphere volcanic history from two Antarctic ice cores, *J. Geophys. Res.*, *102*(D14), 16,761–16,771.
- Cole-Dai, J., D. Ferris, A. Lanciki, J. Savarino, M. Baroni, and M. H. Thiemens (2009), Cold decade (AD 1810–1819) caused by Tambora (1815) and another (1809) stratospheric volcanic eruption, *Geophys. Res. Lett.*, *36*, L22703, doi:10.1029/2009GL040882.
- Cole-Dai, J. H., E. Mosley-Thompson, S. P. Wight, and L. G. Thompson (2000), A 4100-year record of explosive volcanism from an East Antarctica ice core, *J. Geophys. Res.*, *105*(D19), 24,431–24,441.
- Delmas, R. J., S. Kirchner, J. M. Palais, and J. R. Petit (1992), 1000 years of explosive volcanism recorded at the South-Pole, *Tellus Ser. B*, *44*(4), 335–350.

- Eissen, J. P., M. Monzier, and C. Robin (1994), The forgotten volcanic eruption of Kuwae, *Recherche*, 25(270), 1200–1202.
- Esper, J., U. Buntgen, M. Timonen, and D. C. Frank (2012), Variability and extremes of northern Scandinavian summer temperatures over the past two millennia, *Global Planet. Change*, 88–89, 1–9, doi:10.1016/j.gloplacha.2012.01.006.
- Ferris, D. G., J. Cole-Dai, A. R. Reyes, and D. M. Budner (2011), South Pole ice core record of explosive volcanic eruptions in the first and second millennia AD and evidence of a large eruption in the tropics around 535 AD, *J. Geophys. Res.*, 116, D17308, doi:10.1029/2011JD015916.
- Fischer, E. M., J. Luterbacher, E. Zorita, S. F. B. Tett, C. Casty, and H. Wanner (2007), European climate response to tropical volcanic eruptions over the last half millennium, *Geophys. Res. Lett.*, 34, L05707, doi:10.1029/2006GL027992.
- Gao, C. H., L. Oman, A. Robock, and G. L. Stenchikov (2007), Atmospheric volcanic loading derived from bipolar ice cores: Accounting for the spatial distribution of volcanic deposition, *J. Geophys. Res.*, 112, D09109, doi:10.1029/2006JD007461.
- Gao, C. C., A. Robock, and C. Ammann (2008), Volcanic forcing of climate over the past 1500 years: An improved ice core-based index for climate models, *J. Geophys. Res.*, 113, D23111, doi:10.1029/2008JD010239.
- Gao, C. C., A. Robock, S. Self, J. B. Witter, J. P. Steffenson, H. B. Clausen, M. L. Siggaard-Andersen, S. Johnsen, P. A. Mayewski, and C. Ammann (2006), The 1452 or 1453 AD Kuwae eruption signal derived from multiple ice core records: Greatest volcanic sulfate event of the past 700 years, *J. Geophys. Res.*, 111, D12107, doi:10.1029/2005JD006710.
- Hegerl, G. C., T. J. Crowley, M. Allen, W. T. Hyde, H. N. Pollack, J. Smerdon, and E. Zorita (2007), Detection of human influence on a new validated 1500-year temperature reconstruction, *J. Clim.*, 20, 650–666, doi:10.1175/JCLI4011.1.
- Hegerl, G. C., T. J. Crowley, W. T. Hyde, and D. J. Frame (2006), Climate sensitivity constrained by temperature reconstructions over the past seven centuries, *Nature*, 440(7087), 1029–1032, doi:10.1038/nature04679.
- Hogg, A., D. J. Lowe, J. Palmer, G. Boswijk, and C. B. Ramsey (2012), Revised calendar date for the Taupo eruption derived by C-14 wiggle-matching using a New Zealand kauri C-14 calibration data set, *Holocene*, 22(4), 439–449, doi:10.1177/0959683611425551.
- Jenk, T. M., S. Zsidat, D. Bolius, M. Sigl, H. W. Gaggeler, L. Wacker, M. Ruff, C. Barbante, C. F. Boutron, and M. Schwikowski (2009), A novel radiocarbon dating technique applied to an ice core from the Alps indicating late Pleistocene ages, *J. Geophys. Res.*, 114, D14305, doi:10.1029/2009JD011860.
- Jiang, S., J. Cole-Dai, Y. S. Li, D. G. Ferris, H. M. Ma, C. L. An, G. T. Shi, and B. Sun (2012), A detailed 2840 year record of explosive volcanism in a shallow ice core from Dome A, East Antarctica, *J. Glaciol.*, 58(207), 65–75, doi:10.3189/2012JoG11J138.
- Jones, P. D., K. R. Briffa, and F. H. Schweingruber (1995), Tree-ring evidence of the widespread effects of explosive volcanic-eruptions, *Geophys. Res. Lett.*, 22(11), 1333–1336.
- Kekonen, T., J. Moore, P. Peramaki, and T. Martma (2005), The Icelandic Laki volcanic tephra layer in the Lomonosovfonna ice core, Svalbard, *Pol. Res.*, 24(1–2), 33–40, doi:10.1111/j.1751-8369.2005.tb00138.x.
- Kuramoto, T., K. Goto-Azuma, M. Hirabayashi, T. Miyake, H. Motoyama, D. Dahl-Jensen, and J. P. Steffensen (2011), Seasonal variations of snow chemistry at NEEM, Greenland, *Ann. Glaciol.*, 52(58), 193–200, doi:10.3189/172756411797252365.
- Kurbatov, A., G. Zielinski, N. Dunbar, P. Mayewski, E. Meyerson, S. Sneed, and K. Taylor (2006), A 12,000 year record of explosive volcanism in the Siple Dome Ice Core, West Antarctica, *J. Geophys. Res.*, 111, D12307, doi:10.1029/2005JD006072.
- Lanciki, A., J. Cole-Dai, M. H. Thiemens, and J. Savarino (2012), Sulfur isotope evidence of little or no stratospheric impact by the 1783 Laki volcanic eruption, *Geophys. Res. Lett.*, 39, L01806, doi:10.1029/2011GL050075.
- Langway, C. C., K. Osada, H. B. Clausen, C. U. Hammer, and H. Shoji (1995), A 10-century comparison of prominent bipolar volcanic events in ice cores, *J. Geophys. Res.*, 100(D8), 16,241–16,247.
- Larsen, L. B., et al. (2008), New ice core evidence for a volcanic cause of the AD 536 dust veil, *Geophys. Res. Lett.*, 35, L04708, doi:10.1029/2007GL032450.
- Littot, G. C., R. Mulvaney, R. Rothlisberger, R. Udisti, E. W. Wolff, E. Castellano, M. De Angelis, M. E. Hansson, S. Sommer, and J. P. Steffensen (2002), Comparison of analytical methods used for measuring major ions in the EPICA Dome C (Antarctica) ice core, *Ann. Glaciol.*, 35, 299–305, doi:10.3189/172756402781817022.
- Lowe, D. J., and W. P. de Lange (2000), Volcano-meteorological tsunamis, the c. AD 200 Taupo eruption (New Zealand) and the possibility of a global tsunami, *Holocene*, 10(3), 401–407, doi:10.1191/095968300670392643.
- Mann, M. E., J. D. Fuentes, and S. Rutherford (2012), Underestimation of volcanic cooling in tree-ring-based reconstructions of hemispheric temperatures, *Nat. Geosci.*, 5(3), 202–205, doi:10.1038/ngeo1394.
- McConnell, J. R., R. Edwards, G. L. Kok, M. G. Flanner, C. S. Zender, E. S. Saltzman, J. R. Banta, D. R. Pasteris, M. M. Carter, and J. D. W. Kahl (2007), 20th-century industrial black carbon emissions altered arctic climate forcing, *Science*, 317(5843), 1381–1384, doi:10.1126/science.1144856.
- McConnell, J. R., G. W. Lamorey, S. W. Lambert, and K. C. Taylor (2002), Continuous ice-core chemical analyses using inductively Coupled Plasma Mass Spectrometry, *Environ. Sci. Technol.*, 36(1), 7–11, doi:10.1021/es011088z.
- McGwire, K. C., K. C. Taylor, J. R. Banta, and J. R. McConnell (2011), Identifying annual peaks in dielectric profiles with a selection curve, *J. Glaciol.*, 57(204), 763–769.
- Miller, G. H., et al. (2012), Abrupt onset of the Little Ice Age triggered by volcanism and sustained by sea-ice/ocean feedbacks, *Geophys. Res. Lett.*, 39, L02708, doi:10.1029/2011GL050168.
- Monzier, M., C. Robin, and J. P. Eissen (1994), Kuwae (approximate-to-1425 ad) - the forgotten caldera, *J. Volcanol. Geotherm. Res.*, 59(3), 207–218, doi:10.1016/0377-0273(94)90091-4.
- Moore, J. C. (1993), High-resolution dielectric profiling of ice cores, *J. Glaciol.*, 39(132), 245–248.
- Morse, D. L., D. D. Blankenship, E. D. Waddington, and T. A. Neumann (2002), A site for deep ice coring in West Antarctica: results from aerogeophysical surveys and thermo-kinematic modeling, *Ann. Glaciol.*, 35, 36–44, doi:10.3189/172756402781816636.
- Oladottir, B. A., G. Larsen, and O. Sigmarsson (2011), Holocene volcanic activity at Grimsvotn, Bardarbunga and Kverkfjoll subglacial centres beneath Vatnajökull, Iceland, *Bull. Volcanol.*, 73(9), 1187–1208, doi:10.1007/s00445-011-0461-4.
- Oppenheimer, C. (2003a), Climatic, environmental and human consequences of the largest known historic eruption: Tambora volcano (Indonesia) 1815, *Prog. Phys. Geogr.*, 27(2), 230–259, doi:10.1191/0309133303pp379ra.
- Oppenheimer, C. (2003b), Ice core and palaeoclimatic evidence for the timing and nature of the great mid-13th century volcanic eruption, *Int. J. Climatol.*, 23(4), 417–426, doi:10.1002/joc.891.
- Palmer, A. S., T. D. van Ommen, M. A. J. Curran, V. Morgan, J. M. Souney, and P. A. Mayewski (2001), High-precision dating of volcanic events - (AD 1301-1995) using ice cores from Law Dome, Antarctica, *J. Geophys. Res.*, 106(D22), 28,089–28,095.
- Pang, K. D. (1993), Climatic impact of the mid-fifteenth century Kuwae caldera formation, as reconstructed from historical and proxy data, *Eos Trans. AGU*, 74, 106.
- Pasteris, D. R., J. R. McConnell, and R. Edwards (2012), High-Resolution, Continuous Method for Measurement of Acidity in Ice Cores, *Environ. Sci. Technol.*, 46(3), 1659–1666, doi:10.1021/es202668n.
- Pedro, J. B., T. D. van Ommen, S. O. Rasmussen, V. I. Morgan, J. Chappellaz, A. D. Moy, V. Masson-Delmotte, and M. Delmotte (2011), The last deglaciation: timing the bipolar seesaw, *Clim. Past*, 7(2), 671–683, doi:10.5194/cp-7-671-2011.
- Plummer C. T., M. A. J. Curran, T. D. van Ommen, S. O. Rasmussen, A. D. Moy, T. R. Vance, H. B. Clausen, B. M. Vinther, and P. A. Mayewski (2012), An independently dated 2000-yr volcanic record from Law Dome, East Antarctica, including a new perspective on the dating of the c. 1450s eruption of Kuwae, Vanuatu, *Clim. Past Discuss.*, 8, 1567.
- Rasmussen, S., et al. (2006), A new Greenland ice core chronology for the last glacial termination, *J. Geophys. Res.*, 111, D06102, doi:10.1029/2005JD006079.
- Ren, J. W., C. J. Li, S. G. Hou, C. D. Xiao, D. H. Qin, Y. S. Li, and M. H. Ding (2010), A 2680 year volcanic record from the DT-401 East Antarctic ice core, *J. Geophys. Res.*, 115, D11301, doi:10.1029/2009JD012892.
- Riede, F. (2008), The Laacher See-eruption (12,920 BP) and material culture change at the end of the Allerød in northern Europe, *J. Archaeol. Sci.*, 35(3), 591–599, doi:10.1016/j.jas.2007.05.007.
- Robock, A. (2000), Volcanic eruptions and climate, *Rev. Geophys.*, 38(2), 191–219.
- Salzer, M. W., and M. K. Hughes (2007), Bristlecone pine tree rings and volcanic eruptions over the last 5000 yr, *Quat. Res.*, 67(1), 57–68, doi:10.1016/j.yqres.2006.07.004.
- Sato, M., J. E. Hansen, M. P. McCormick, and J. B. Pollack (1993), Stratospheric aerosol optical depths, 1850–1990, *J. Geophys. Res.*, 98(D12), 22,987–22,994, doi:10.1029/93jd02553.
- Savarino, J., A. Romero, J. Cole-Dai, S. Bekki, and M. H. Thiemens (2003), UV induced mass-independent sulfur isotope fractionation in stratospheric volcanic sulfate, *Geophys. Res. Lett.*, 30(21), 2131, doi:10.1029/2003GL018134.
- Simkin, T., and L. Siebert (1994), *Volcanos of the World*, 349 pp., Geoscience, Tucson, Ariz.
- Sommer, S., D. Wagenbach, R. Mulvaney, and H. Fischer (2000), Glaciochemical study spanning the past 2 kyr on three ice cores from Dronning Maud Land, Antarctica 2. Seasonally resolved chemical records, *J. Geophys. Res.*, 105(D24), 29,423–29,433, doi:10.1029/2000JD900450.

- Sparks, R. J., W. H. Melhuish, J. W. A. McKee, J. Ogden, J. G. Palmer, and B. P. J. Molloy (1995), C-14 calibration in the southern hemisphere and the date of the last Taupo eruption: Evidence from tree-ring sequences, *Radiocarbon*, *37*(2), 155–163.
- Steig, E. J., D. P. Schneider, S. D. Rutherford, M. E. Mann, J. C. Comiso, and D. T. Shindell (2009), Warming of the Antarctic ice-sheet surface since the 1957 International Geophysical Year, *Nature*, *457*(7228), 454–459, doi:10.1038/nature07669.
- Steig, E. J., et al. (2005), High-resolution ice cores from USITASE (West Antarctica): development and validation of chronologies and determination of precision and accuracy, *Ann. Glaciol.*, *41*, 77–84.
- Stenni, B., M. Proposito, R. Gragnani, O. Flora, J. Jouzel, S. Falourd, and M. Frezzotti (2002), Eight centuries of volcanic signal and climate change at Talos Dome (East Antarctica), *J. Geophys. Res.*, *107*(D9), 4076, doi:10.1029/2000JD000317.
- Stuiver, M., and B. Becker (1993), High-precision decadal calibration of the radiocarbon time scale, AD 1950–6000 BC, *Radiocarbon*, *35*(1), 35–65.
- Taylor, K. C., R. B. Alley, G. W. Lamorey, and P. Mayewski (1997), Electrical measurements on the Greenland Ice Sheet Project 2 core, *J. Geophys. Res.*, *102*(C12), 26,511–26,517, doi:10.1029/96jc02500.
- Taylor, K., et al. (2004), Dating the Siple Dome (Antarctica) ice core by manual and computer interpretation of annual layering, *J. Glaciol.*, *50*(170), 453–461, doi:10.3189/172756504781829864.
- Thomas, M. A., C. Timmreck, M. A. Giorgetta, H. F. Graf, and G. Stenchikov (2009), Simulation of the climate impact of Mt. Pinatubo eruption using ECHAM5-Part 1: Sensitivity to the modes of atmospheric circulation and boundary conditions, *Atmos. Chem. Phys.*, *9*(2), 757–769.
- Thordarson, T., and G. Larsen (2007), Volcanism in Iceland in historical time: Volcano types, eruption styles and eruptive history, *J. Geodyn.*, *43*(1), 118–152, doi:10.1016/j.jog.2006.09.005.
- Thordarson, T., and S. Self (2003), Atmospheric and environmental effects of the 1783–1784 Laki eruption: A review and reassessment, *J. Geophys. Res.*, *108*(D1), 4011, doi:10.1029/2001JD002042.
- Trautetter, F., H. Oerter, H. Fischer, R. Weller, and H. Miller (2004), Spatio-temporal variability in volcanic sulphate deposition over the past 2 kyr in snow pits and firn cores from Amundsenisen, Antarctica, *J. Glaciol.*, *50*(168), 137–146.
- Vinther, B. M., et al. (2006), A synchronized dating of three Greenland ice cores throughout the Holocene, *J. Geophys. Res.*, *111*(D13), D13102, doi:10.1029/2005JD006921.
- Weller, R., J. Woltjen, C. Piel, R. Resenberg, D. Wagenbach, G. Konig-Langlo, and M. Kriews (2008), Seasonal variability of crustal and marine trace elements in the aerosol at Neumayer station, Antarctica, *Tellus Ser. B*, *60*(5), 742–752, doi:10.1111/j.1600-0889.2008.00372.x.
- Williams, M. A. J., S. H. Ambrose, S. van der Kaars, C. Ruehlemann, U. Chattopadhyaya, J. Pal, and P. R. Chauhan (2009), Environmental impact of the 73 ka Toba super-eruption in South Asia, *Palaeogeogr. Palaeoclim. Palaeoecol.*, *284*(3–4), 295–314, doi:10.1016/j.palaeo.2009.10.009.
- Wilson, C. J. N. (1993), Stratigraphy, chronology, styles and dynamics of late quaternary eruptions from Taupo volcano, New-Zealand, *Philos. Trans. R. Soc. London Ser. A*, *343*(1668), 205–306, doi:10.1098/rsta.1993.0050.
- Wilson, C. J. N., and G. P. L. Walker (1985), The Taupo eruption, New-Zealand. I. General aspects, *Philos. Trans. R. Soc. London Ser. A*, *314*(1529), 199, doi:10.1098/rsta.1985.0019.
- Wilson, C. J. N., N. N. Ambraseys, J. Bradley, and G. P. L. Walker (1980), A new date for the Taupo eruption, New Zealand, *Nature*, *288*(5788), 252–253, doi:10.1038/288252a0.
- Zielinski, G. A. (1995), Stratospheric loading and optical depth estimates of explosive volcanism over the last 2100 years derived from the Greenland-Ice-Sheet-Project-2 ice core, *J. Geophys. Res.*, *100*(D10), 20,937–20,955, doi:10.1029/95jd01751.
- Zielinski, G. A., P. A. Mayewski, L. D. Meeker, S. Whitlow, M. S. Twickler, M. Morrison, D. A. Meese, A. J. Gow, and R. B. Alley (1994), Record of volcanism since 7000–BC from the GISP2 Greenland ice core and implications for the volcano-climate system, *Science*, *264*(5161), 948–952.